Hybrid q-Rung Orthopair Fuzzy Sets Based CoCoSo Model for Floating Offshore Wind Farm Site Selection in Norway

Muhammet Deveci, Dragan Pamucar, Umit Cali, *Member*, *IEEE*, Emre Kantar, Konstanze Kölle, and John O. Tande

***Abstract*—Unlocking offshore wind farms' high energy generation potential requires a comprehensive multi-disciplinary analysis that consists of intensive technical, economic, logistical, and environmental investigations. Offshore wind energy projects have high investment volumes that make it essential to conduct extensive site selection to ensure feasible investment decisions that reduce the potential financial risks. Depending on the scenario and circumstances, a ranking of alternative offshore wind energy projects helps to prioritise the investment decisions. Decision-making algorithms based on expert knowledge can support the prioritisation and thus alleviate the work load for investment decisions in the future. The case study considered here is to find the best site for a floating offshore wind farm in Norway from four pre-selected alternatives: Utsira Nord, Stadthavet, Frøyabanken, and Træna Vest. We propose a hybrid decision-making model as a combined compromised solution (CoCoSo) based on the q-rung orthopair fuzzy sets (q-ROFSs) including the weighted q-rung orthopair fuzzy Hamacher average (Wq-ROFHA) and the weighted q-rung orthopair fuzzy Hamacher geometric mean (Wq-ROFHGM) operators. In this model, the q-ROFSs based full consistency method (FUCOM) is introduced as a new methodology to determine the weights of the decision criteria. The results of the proposed model show that the best site among the investigated four alternatives is A_1: Utsira Nord. A sensitivity analysis has verified the stability of the proposed decision-making model.**

***Index Terms*—Decision-making, q-rung orthopair fuzzy sets, Fuzzy hamacher, site selection, offshore wind farm, FUCOM.**

I. Introduction

WIND energy is rapidly developing and is expected to be an essential part of the future energy system. Most of today's capacity is installed on land (620 GW out of 650 GW), whereas offshore wind resources represent a massive untapped potential [1]. Wind can supply about 35% of the global electricity demand by 2050 with 5000 GW land-based wind capacity and 1000 GW offshore wind capacity [2]. The most ambitious scenario defined by the European Commission suggests 450 GW offshore wind capacity in Europe by 2050 [3]. To be successful, however, cost-competitive solutions must be developed.

In 2019, 502 offshore wind turbines (OWT) across ten offshore wind farms were connected to the grid all over Europe. This upgrade translated into an additional 3627-MW gross capacity, increasing the total number of grid-tied OWT to 5047 and the total installed offshore wind power capacity to 22072 MW across 12 countries, as shown in Fig. 1 [4]. The UK, Denmark and Belgium set national installation records in 2019 by installing additional capacities of 1764 MW, 374 MW, and 370 MW, respectively [4]. Norway, on the other hand, did not connect additional offshore turbines to the grid in the same year. However, the pre-commercial 88-MW Hywind Tampen floating wind farm reached Final Investment Decision (FID) in 2019 with an expected commissioning date in 2022 [4].

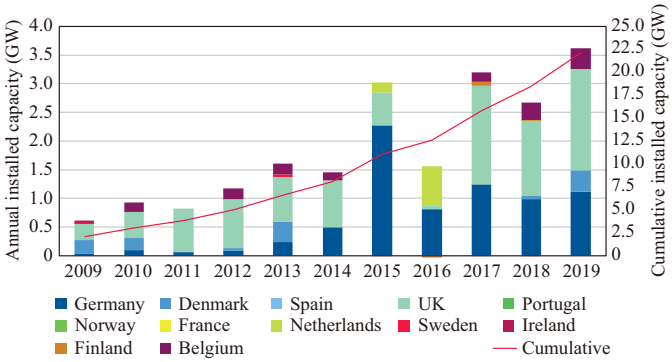

Fig. 1. Annual offshore wind installations in Europe (left axis) and cumulative installed capacity (right axis) [4]. (Data source: WindEurope, used with permission.)

A recent review considers site selection as the most important criterion for successful investments in offshore wind

Manuscript received October 14, 2021; revised November 23, 2021; accepted December 20, 2021. Date of online publication January 5, 2022; date of current version July 10, 2022. This work has been prepared as part of the Norwegian Research Centre on Wind Energy (NorthWind) and the project Research on Smart Operation Control Technologies for Offshore Wind Farms (CONWIND). NorthWind (2021-2029) is a Centre for Environmental-friendly Energy Research co-financed by the Research Council of Norway (contract 321954). CONWIND (2020-2022) is a Norwegian-Chinese collaboration project on offshore wind energy co-financed by the Research Council of Norway (contract 304229).

M. Deveci is with the Department of Industrial Engineering, Turkish Naval Academy, National Defence University, Istanbul 34940, Turkey.

D. Pamucar is with the Department of Operations Research and Statistics, Faculty of Organizational Sciences, University of Belgrade, Belgrade, Serbia.

U. Cali is with the Department of Electric Power Engineering, Norwegian University of Science and Technology, Trondheim NO-7491, Norway.

E. Kantar is with the Department of Electric Power Technology, SINTEF Energy Research, Trondheim NO-7491, Norway.

K. Kölle (corresponding author, email: konstanze.koelle@sintef.no; ORCID: https://orcid.org/0000-0002-6680-5392) and J. O. Tande are with the Department of Energy Systems, SINTEF Energy Research, Trondheim NO-7034, Norway.

DOI: 10.17775/CSEEJPES.2021.07700

power [5]. Most published studies on offshore site selection focus on single courtries [6]–[22]. Only a few studies consider larger areas such as the Baltic States [23], the North Sea [24], and Europe [25]. No previous study in this category focused particularly on floating offshore wind farms. However, a study on offshore renewable energy platforms considers floating wind turbines together with wave and tidal power [25].

The above-listed studies on the site selection for offshore wind farms include three [18], [21], [25] to 55 [19] pre-selected alternatives from which the best suited site is chosen using decision-making algorithms. Fuzzy-based algorithms are applied to consider expert judgement in the decision process. Multi-criteria decision-making (MCDM) is the most common methodology for site selection because various main criteria can be ranked as a group including their sub-criteria. Relevant main criteria for offshore site selection are technical, economic, social, and environmental. However, not all studies that analyse the offshore site selection include both main and sub-criteria. The number of considered criteria varies tremendously from three main-criteria with six sub-criteria [23] to seven main-criteria with 23 sub-criteria [8]. Depending on the decision-making algorithm, no differentiation between main- and sub-criteria is applied. A meta-analysis investigates the importance of various criteria for the site selection of offshore wind farms [26]. Energy economic aspects are of particular importance when judging sites for wind farms. Such evaluations can be in the form of a cost-benefit analysis [12], [15]–[17], the levelised cost of energy (LCOE) [13], [18], [22], [24], or cost [Operational Expenditures (OPEX) and Operational Expenditures (CAPEX)] [8], [14], [23]. However, several of the mentioned site-selection studies do not include energy economic considerations.

Exploiting the high potential of offshore wind energy resources requires a well-structured multi-disciplinary analysis that consists of technical, economic, logistical, ecological and environmental evaluations. Commercial offshore wind energy investments are realised with considerably high investment costs. They can be effectuated by a number of experienced experts who can execute a comprehensive site selection strategy and methods to make the best available investment decision. The decision-making convention proposed in this study can be considered a handy decision-support tool that can assist experts and project investors in making better decisions. In this perspective, this study proposes a q-Rung Orthopair fuzzy sets (q-ROFSs) based multi-criteria decision-making (MCDM) model to assess and rank Norway's most promising floating offshore wind sites.

The theory of fuzzy sets (FSs) known as a type-1 fuzzy set, which is represented by the degree of membership, was proposed by Zadeh [27]. Fuzzy sets have been successfully used in many applications to address ambiguous and imprecise information [28]. However, the modelling tools of FSs have been limited to handle vague and inexact information in which two or more sources of uncertainty arise simultaneously. Consequently, different generalisations and extensions of fuzzy sets in the literature have been introduced by various researchers [29] such as rough sets [30], intuitionistic fuzzy sets [31], type-2 fuzzy sets [32], interval type-2 fuzzy sets [33], hesitant fuzzy sets [34], Pythagorean fuzzy sets (PFSs) [35], etc. In addition, various fuzzy sets have been applied to decision-making problems such as picture fuzzy set [36], spherical fuzzy sets [37], and bipolar soft sets [38]. These generalised fuzzy forms have been applied specifically in many real-world MCDM problems.

One such generalisation is intuitionistic fuzzy sets (IFSs) which Atanassov introduced [31]. Intuitionistic fuzzy sets are characterised by a degree of membership and non-membership functions with the condition that the sum of these degrees is less than or equal to 1. Nevertheless, it still appears that the applicable region of IFSs is triangular, and access is limited (see Fig. 2). For example, when decision-makers present their evaluation for the degree of membership of the element with 0.8 and degree of non-membership of the element with 0.5, IFSs cannot be effective because the sum of these two values $(0.8 + 0.5 = 1.3)$ is greater than 1.

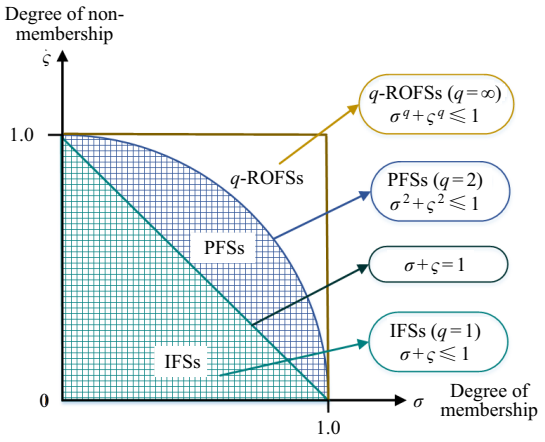

Fig. 2. Comparison of spaces of different fuzzy membership grades.

To overcome this issue and extend the searching space, Yager and Abbasov [35] introduced the idea of Pythagorean fuzzy sets (PFSs), which are general forms of the IFSs, characterised by the degree of membership and non-membership functions with the condition that the sum of these degrees is less than or equal to 1 [39]. For example, let an expert evaluation $(0.8, 0.5)$ be handled with PFSs as $0.8^2 + 0.5^2 = 0.89$. While this situation is not possible with IFS as $0.8 + 0.5 > 1$, PFSs effectively overcome it (see Fig. 2).

q-Rung Orthopair fuzzy sets that Yager [40] has recently introduced present an extension of IFSs and PFSs. The geometric interpretations of the space of IFSs, PFSs, and q-ROFSs are illustrated in Fig. 2. The sum of the qth powers of the membership and non-membership degrees of q-ROFSs is limited to one [41]. As the rung q increases, the allowable area of the orthopyres escalates, and, therefore, more orthopyres meet the constraints. As a result, q-ROF numbers give us the flexibility to express a broader scope of fuzzy information [42]. Recently, there has been a growing interest in the q-ROFSs such as [43]–[45]. Consequently, we prefer q-ROFSs in this study because of the advantage of the freedom to choose the power degree. This study proposes a q-ROFSs based integrated full consistency method (FUCOM) and combined

compromised solution (CoCoSo) decision-making model to better handle vagueness and imprecise information.

The primary aim of this study is to select the best site for a floating offshore wind farm (OWF) among four alternatives in Norway, which is proposed to be utilised as an advanced decision-support tool for making feasible investment decisions. To achieve this aim, a novel hybrid MCDM model including q-ROF FUCOM and CoCoSo is proposed. In addition, there is no other study in the literature that applied any MCDM model for floating OWF.

The contributions of this study are as follows: (i) A novel hybrid MCDM is proposed for the site selection of the OWF. This hybrid MCDM model is named q-ROF FUCOM and q-ROF CoCoSo, respectively, providing alternative evaluations of subjective and objective expert perspectives. (ii) q-ROFSs technique is implemented to handle the uncertainty in experts' assessments. (iii) A modified q-ROF CoCoSo is proposed to rank the alternative OWF sites. (iv) A q-ROF FUCOM is used to calculate the criteria weights. (v) A Norwegian case study for the floating offshore wind farms is presented to illustrate the feasibility of the proposed model.

This study presents a hybrid multi-criteria methodology based on improving the CoCoSo method using weighted q-rung orthopair fuzzy Hamacher functions and extending the FUCOM method in a q-rung orthopair fuzzy environment. The original CoCoSo model uses comparisons based on weighted averaging of alternative values. Weighted averaging is performed in two ways. The first method involves the application of weighted sum averaging (WSM), while the second method involves the calculation of the overall relative importance of alternatives using weighted geometric averaging (WPM). After defining the weighted value, the values are aggregated to obtain a unique ranking index. Aggregation is done through the application of three aggregation strategies that are applied to each given alternative.

In general, we can conclude that the described procedure is based on a combination of compromise strategies. The weighted values of the criterion functions obtained by applying WSM and WPM have a decisive influence on the final ranking of alternatives. Both models (WSM and WPM) give objective values of the criterion functions if the estimates of the alternatives in the home matrix are uniform. However, there is a disproportionate increase in the criterion function in cases where there are extreme deviations in the values of the most influential criteria. One of the reasons for such variations is the character of the WSM function, which is linear. This is especially important in cases where some limit values of the home matrix can distort the result of aggregation and thus lead to incorrect prioritization of alternatives, which can further lead to wrong decisions. Deviations of the input values in the home matrix can occur for several reasons. Some of them are measurement errors and biased expert assessments (either intentional or unintentional). Another disadvantage of WSM and WPM aggregation is ignoring the interaction between the criteria.

However, decision making in real systems requires the elimination of such anomalies in decision-making tools. Therefore, it is necessary to incorporate mechanisms/algorithms into decision support systems to understand attribute relationships rationally and eliminate the impact of extreme/awkward data. To overcome the described problem in the CoCoSo model Hamacher aggregation functions are proposed; i.e., the application of weighted q-rung orthopair fuzzy Hamacher average (Wq-ROFHA) and weighted q-rung orthopair fuzzy Hamacher geometric mean (Wq-ROFHGM) functions. These aggregation functions enable the recognition of connections between criteria and their fusion into a unique criterion function. However, to the best authors' knowledge, there is no research in the literature showing the integration of Hamacher functions into the CoCoSo model. Therefore, this study's logical goal and motivation are to show that the Hamacher operator can be used to fuse criterion functions in the home decision matrix of the CoCoSo model. The main advantages of the improved CoCoSo model are highlighted below: the model enables flexible decision making; the model has the flexibility to simulate risk in decision making; and the model enables the verification of the robustness of the results through the variation of the parameters q and Υ and the verification of their influence on the final decision.

The second segment of the multi-criteria framework is the advanced FUCOM method. The improvement of the FUCOM method is shown through the extension of the nonlinear model in q-rung orthopair fuzzy environment. Q-rung orthopair fuzzy FUCOM methodology enables the objective perception of uncertainty during pairwise comparisons of criteria, allows the definition of objective values of criteria with a small number of comparisons, i.e., requires only $n-1$ comparison of criteria, provides the possibility of defining the quality of the obtained values of weight coefficients by defining a coefficient that shows the deviation from the ideal values of the weight of the criteria, and the model fully respects mathematical transitivity during comparisons in pairs of criteria.

II. Background

Background information for the types of recent OWT foundations and their share in today's market is presented here. In addition, the overall efficiency of a wind turbine considering the sources of the losses are presented along with our assumptions for further analyses in this work.

A. Offshore Wind Turbine Foundations

Figure 3(a) illustrates various fixed-bottom foundations and support structure types for OWT according to the appropriate water depths.

Gravity-based foundations and monopiles are suitable for shallow waters up to 35-m depth where most OWTs are currently installed [46]. The monopile foundation, a hollow steel tube hammered into the seabed, is the most preferred option for shallow waters due to its simplicity and robustness [47]. The gravity-based foundation merely relies on its own weight to achieve firm support for OWTs and requires a stable seabed. Therefore, it is only economically feasible in very shallow waters [46].

When installing wind turbines in deeper water (30–80 m), however, such monopile and gravity-based foundations become less attractive as a disproportional amount of material

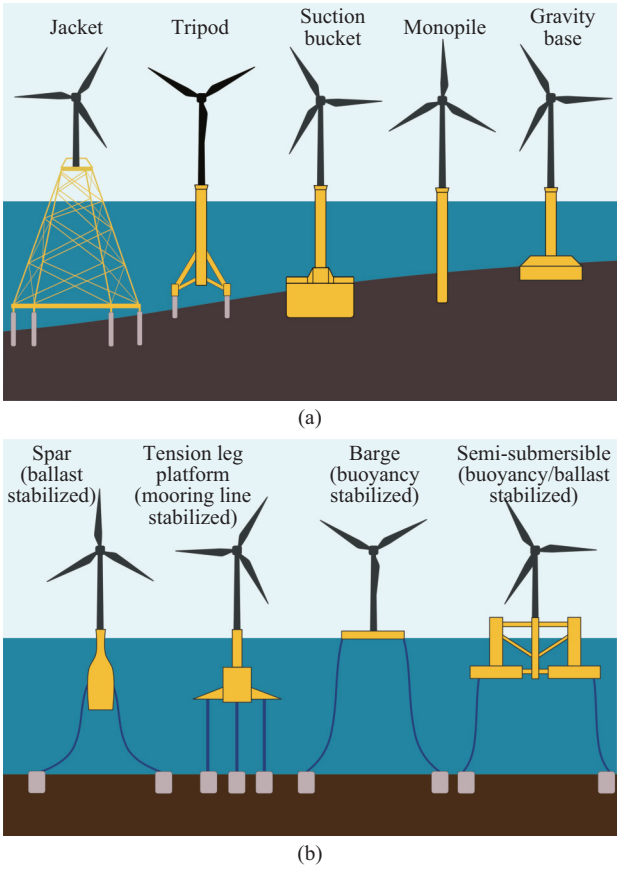

Fig. 3. Different foundation types for offshore wind turbines: (a) non-floating, bottom-fixed turbines. (b) floating turbines.

is needed for it to withstand the more severe loading. More complex types of foundations then become more attractive. Suction buckets, tripods, and jackets are the other foundation types for bottom-fixed structures with various advantages and disadvantages that influence the final decision making. Feasibility, costs, construction limitations and geotechnical stability are among the most critical factors. For example, as jackets are composed of many tubular elements connected in welded nodes, the production costs of jackets are relatively high.

Monopiles were the most chosen substructure type in 2019, with a staggering 70% of all newly installed OWT [4]. With the new installations in 2019, monopiles still top the list, with 4258 units (81%) to date (including all with and without grid connection). Jackets were the second most popular foundation accounting for 29% of all substructures installed in 2019, increasing its accumulated share to 8.9% [4]. Gravity-based foundations (5.7%) and tripods (3.9%) follow jackets in the cumulative sum [4].

Floating foundations are favoured over bottom-fixed solutions at deep waters ($>$ 80 m) [46]. Spar, tension leg platform, barge, and semi-submersible are the primary floating structure types, as illustrated in Fig. 3(b). To date, only nine grid-connected floating OWTs (out of 5258 OWT $\approx$ 0.17%) are in operation: six spars, one barge and two semi-submersibles [4]. Although the number of floating OWTs may seem rather low, the trend is climbing: the total share of floating OWT in 2016 was only 0.02% whereas it is currently 0.17%. With the growing interest in utilizing the wind potential at deeper waters, the number of floating substructures is likely to increase significantly in the coming years. According to a study by IEA [1], 80% of the global wind resource is available at sites with a water depth between 60 and 2000 m.

B. Wind Power Output

The average power that can be harvested from the wind (P_w), striking on a surface with area A (e.g., equal to the rotor swept area of a wind turbine [m^2]) is calculated by:

$$P_w = \frac{1}{2}\rho A v^3 \tag{1}$$

where ρ is the air density [kg/m^3], and v is the wind speed [m/s]. However, the theoretical limit to the maximum extracted power from the wind $P_{w,e}$ is 59.3% according to Betz's law. Modern wind turbines can extract as much wind power as 45%–50%, which is close to the theoretical limit [48]. One of the main loss mechanisms that determine $P_{w,e}$ are aerodynamic (turbine blades) and mechanical losses (gearbox, rotating parts, etc.) caused by the wind turbine. Besides, wind power production is further inhibited as the placement of the turbines in a wind farm becomes sub-optimal due to practical and feasibility reasons.

The capacity factor (CF) of a single wind turbine or small-scale wind farm cannot simply be extrapolated to a large wind farm that consists of tens or hundreds of wind turbines. A wake is generated between the front-row and back-row turbines, causing a wind speed deficit. Since wind power is proportional to the cube of wind speed, as shown in (1), substantial exploitable wind energy will be lost in case of a significant deficit in wind speed due to close array spacing. Therefore, there should be enough space between the turbines to extract as much energy as possible from the incoming wind by reducing the wake power losses [49]. Wake power losses can be alleviated by enabling wind speed recovery through the renewal of kinetic energy, particularly in the vertical direction for large arrays [48]. Besides choosing a farm layout with sufficient turbine spacing, wind farm flow control which manipulates the wake between wind turbines is investigated to increase the power output during operation [50]. However, several studies suggest that the wind turbine spacing (n) should be no less than 7–10 rotor diameters, D (i.e., the swept area by the blades) to minimise the array losses [48], [51], [52].

The turbine and array losses should then be reflected on P_w such that the extracted power $P_{w,e}$ becomes:

$$P_{w,e} = \frac{1}{2}\rho A v^3 \eta_t \eta_a \tag{2}$$

where η_t and η_a stand for the turbine efficiency and array efficiency, respectively, as illustrated in Fig. 4. As mentioned above, modern large wind turbines offer maximum turbine efficiencies closer to 85% of the Betz limit, i.e., $\eta_{t_{\max}} \approx 50\%$.

We fitted the array efficiencies for different turbine spacing and array sizes provided in [53] to the following mathematical expression as a function of the turbine spacing n (by a factor of the rotor diameter D), as plotted in Fig. 5:

$$\eta_a = a e^{b\frac{\pi}{4n^2}} \tag{3}$$

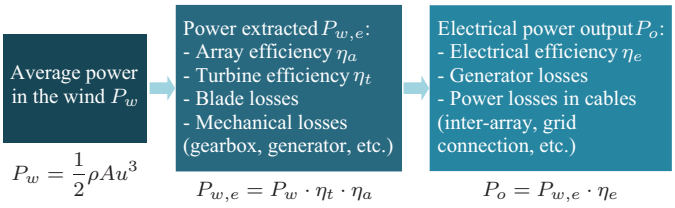

Fig. 4. Overall efficiency of a wind turbine including turbine, array and electrical losses.

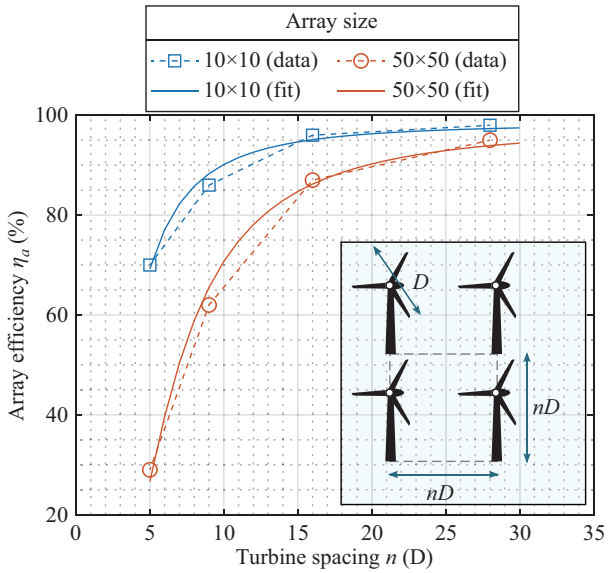

Fig. 5. Influence of turbine spacing on the array efficiency for two different array sizes (10×10 and 50×50).

where $a = 98.42$, $b = -11.19$ for a 10×10 array size while $a = 97.88$, $b = -41.37$ for a 50×50 array size. Dupont *et al*. [48] and Meyers & Meneveau [51] claim 15 D would be a more optimal spacing for extracting the most wind over the conventionally favoured distancing of 7 D. However, resulting electrical losses and CAPEX were not considered in these analyses. Therefore, we chose a 10×10 array size (100 turbines) with an array spacing of $n = 10$ D, as an intermediate value for the analysis performed in the next section. The resulting array efficiency was then calculated to be 90.14%, as can be seen in Fig. 5. There are also losses associated with outages due to faults, repair and service of turbines or the connected grid. These typically account for about 2%–5% of the annual energy output. In this study, however, such losses are disregarded for the sake of simplicity.

Lastly, as depicted in the rightmost category in Fig. 4, electrical losses incurred by the generator and the cable connections (inter-array and grid connections) should also be considered when calculating the electrical power output P_o. The number of wind turbines connected to the grid in a wind farm, array spacing, location-specific parameters (distance to the grid connection point and coast, water depth, average wave height, etc.) determine the total length of inter-array cable connections/types and the total cable length for the grid connection, and hence, determine the total electrical losses. The power losses associated with transmission and distribution, i.e., after the grid connection point, are under the liabilities of transmission and distribution system operators, and therefore are not taken into account. Given the significance of these parameters, a thorough analysis is required to estimate electrical losses for each site. Since the main objective of this work is to determine the best location for an offshore wind farm among four alternatives in Norway (using a decision-making algorithm based on multiple techno-economical, environmental and societal criteria), such a comprehensive task is beyond the scope of this paper. Consequently, electrical losses are assumed to be 2% of the rated power for each site in this work, leading to an electrical efficiency of $\eta_e = 98\%$.

III. Methodology

Making investment decisions, especially for large-scale projects such as OWFs, is a challenging task for companies and other decision-makers. Such investment decisions require multi-disciplinary analysis, accommodating various dimensions such as energy, political, legislative, technical, economic, social and environmental issues. In this study, four Norwegian locations, identified as primary locations for floating offshore wind farm projects, are scrutinised using state-of-the-art decision-making algorithms and the corresponding analysis to support the proposed framework.

A. Site Description

The Norwegian Water Resources and Energy Directorate (NVE) identified potential sites for offshore wind in 2010 [54], as shown in Fig. 6. The pink colour indicates the four sites relevant for floating wind farms, from South to North: Utsira Nord, Stadthavet, Frøyabanken and Træna Vest.

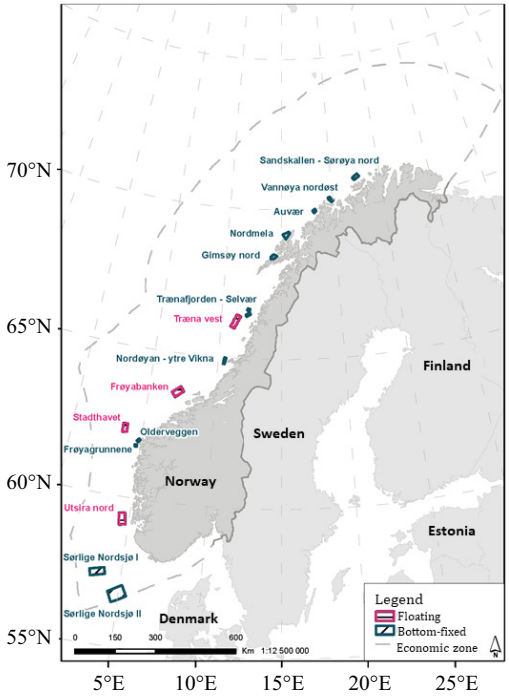

Fig. 6. Identified sites for offshore wind farms in Norway, adapted from [54]. (Data source: NVE, used with permission.)

More detailed analyses of the proposed sites have been conducted and published in a summary report by NVE in 2012 [55], upon which the following information is based.

1) Utsira Nord

Utsira Nord is located in southern Norway, west of Haugesund. Fig. 7(a) shows the coordinates of the area. The area has a total size of 1010 km^2 which makes it the largest among those for floating wind farms. Utsira Nord has a distance of only 22 km to the floating site that lies closest to the coast, settlements and harbours. The proximity to shore has the consequence that wind turbines placed in Utsira Nord can be visible from land.

An installed capacity of 500–1500 MW is considered realistic. However, the maximum installed capacity depends on the grid connection. An installed capacity of 500 MW is possible with the existing infrastructure, and an additional 500 MW should be possible by 2025 [56], while a connection of up to 1500 MW can be examined [57]. Export of the produced power is also possible.

2) Stadthavet

Stadthavet is located 58 km off the coast from Nordfjord. The location is shown in Fig. 7(b) with a an area of 520 km^2. Among all evaluated sites, Stadthavet has the roughest weather conditions with the highest average and 50-year values for both wind speed and wave heights.

The wind conditions permit a capacity of 500–1500 MW. Assuming an installed capacity of 1000 MW, the OWF could not be connected to the regional grid before 2030.

3) Frøyabanken

Frøyabanken is located in Mid-Norway, at a distance of 34 km from the coast. The sea depth and coordinates of the 819 km^2 area are shown in Fig. 7(c).

The wind conditions permit a capacity of 500–1500 MW. Assuming an installed capacity of 1000 MW, the OWF could not be connected to the regional grid before 2030.

4) Træna Vest

Træna Vest is the potential floating site that is located farthest North. The site has a total size of 773 km^2 and is

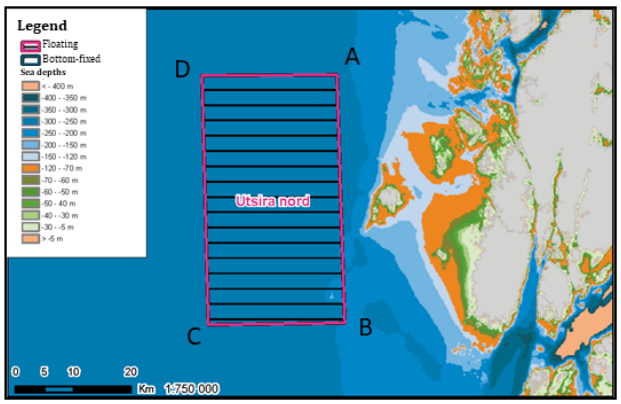

(a) Utsira Nord. Coordinates:

A	4°40′25″E	59°28′56″N
B	4°48′44″E	59°06′18″N
C	4°24′27″E	59°04′10″N
D	4°16′09″E	59°26′53″N

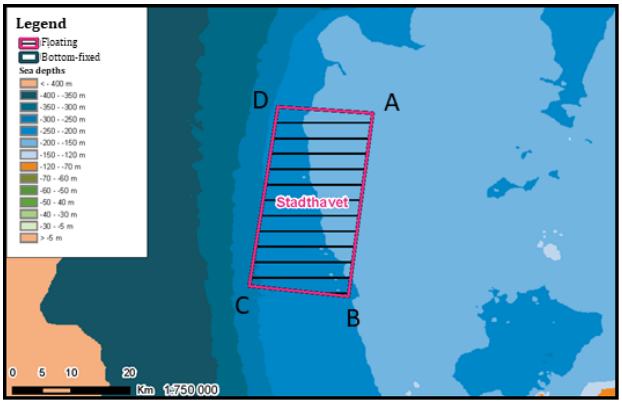

(b) Stadthavet. Coordinates:

A	3°52′44″E	62°25′49″N
B	3°54′12″E	62°08′54″N
C	3°34′44″E	62°08′15″N
D	3°34′01″E	62°24′51″N

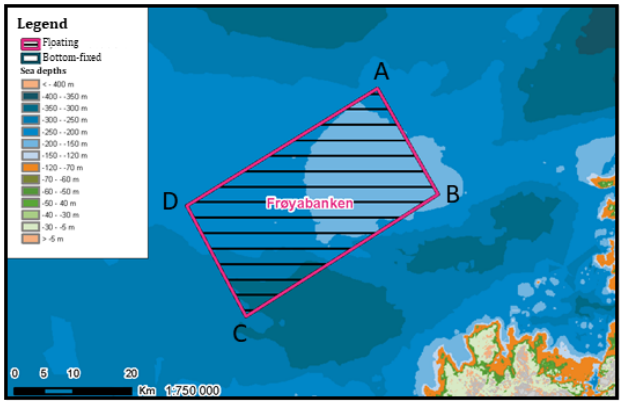

(c) Frøyabanken. Coordinates:

A	7°21′35″E	63°54′02″N
B	7°36′48″E	63°45′03″N
C	7°00′15″E	63°31′45″N
D	6°45′09″E	63°41′09″N

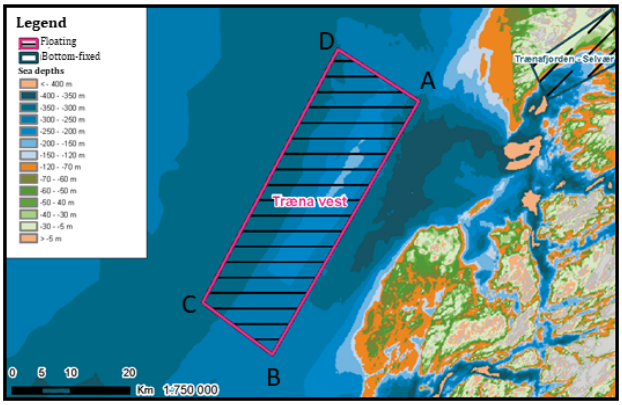

(d) Træna Vest. Coordinates:

A	11°35′31″E	66°23′31″N
B	11°05′31″E	65°59′25″N
C	10°49′01″E	66°03′48″N
D	11°16′14″E	66°27′51″N

Fig. 7. Sea depths at the four OWF sites with coordinates, adapted from [54]. (Data source: NVE, used with permission.)

located 45 km from land. The exact coordinates are shown in Fig. 7(d).

The wind conditions permit a capacity of 500–1500 MW. Assuming an installed capacity of 1000 MW, the OWF could not be connected to the regional grid before 2030.

B. Determination of Decision-making Variables

The decision-making logic relies on a certain set of alternatives and their criteria. The alternatives were four Norwegian sites for OWFs where the floating foundation types were eligible described in the previous section. In this section, the definitions of the influencing criteria are explained. The hierarchical structure of OWF site selection is shown in Fig. 8. The subject associated criteria definitions are investigated under two main groups: 1) techno-economical, 2) environmental and social.

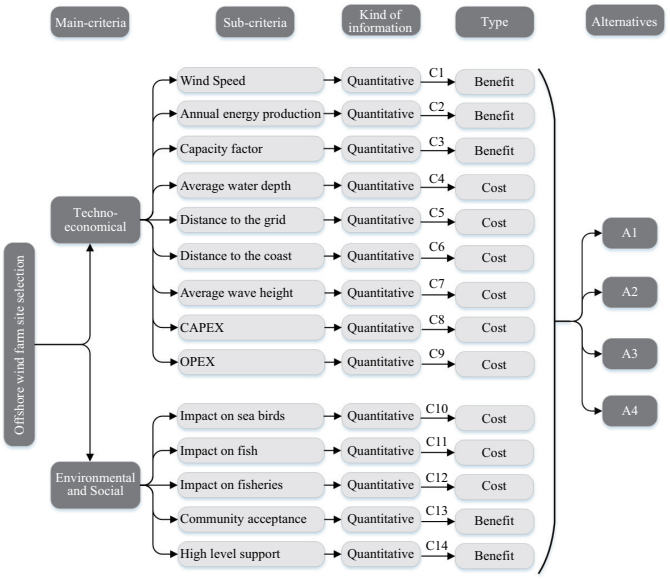

Fig. 8. The decision hierarchy of the OWF site selection problem.

1) Wind speed

Wind speed is one of the most important parameters as technical criterion, which is used to identify the best available wind power project location. The pressure difference occurring in the atmosphere creates the wind flow. Wind power is related to the wind flow or air in motion in terms of kinetic energy. More precisely, wind power generated from the kinetic energy of the wind flow is directly proportional to the cube of the wind speed (see Section II-B).

2) Annual energy production (AEP)

AEP is a measure that represents the amount of electrical energy which can be harvested from a wind turbine, wind farm or an extended region within a year. The AEP is estimated by considering the factors summarised in the previous section and some other impacts such as the efficiency of the power system components, cable length, cable type, location of the wind farm, the layout of the wind turbines. kWh, MWh and GWh are the units to quantify the AEP values.

3) Capacity factor

Ratio between the real or estimated AEP of a wind farm or turbine and the maximum amount of energy that could be generated if the system was be operated with the full load hours (8760 hours a year).

4) Average water depth

Average water depth is calculated as the average for the potential site because the water depth varies within each of the sites. Floating offshore wind turbines are moored to the ground to prevent drifting, and the length of the mooring lines depends on the water depth.

5) Distance to grid connection point and electrical works

Distance to the closest power grid transformer or substation is one of the most influencing parameters that impacts various technical factors such as power losses and economic factors, for example CAPEX figures related to the electrical works like cabling. Power system losses are correlated with the type, length of the cabling and the power system topology of the planned OWF. The closest existing transformer station onshore is used here if this station has capabilities for the additional power from the potential, new OWF.

6) Distance to coast

Distance to coast is vital for construction, operation and decommissioning. During the operational life, the vessel transfer time for maintenance is a significant cost factor. However, details such as locations of suitable harbours were not considered in this study.

7) Average wave height

Average wave height is important due to the accessibility of the OWF for service vessels to perform maintenance. The wave climate also affects the motion of floating wind turbines, the requirements of the mooring system, and the design and tuning of a counteracting control system.

8) CAPEX

CAPEX stands for capital expenditures which describes initial investment costs executed to realise the OWF. The cost of wind turbines, foundations, electrical works, civil works, project development, permits, and other relevant costs can be considered as OWF-specific CAPEX values.

9) OPEX

OPEX stands for operational expenditures which describe the operating costs of the OWF. The cost of operation and maintenance, spare parts, staff salaries, insurance, overhead, and other relevant expenses can be considered OWF-specific OPEX values.

10) Impact on sea birds

The impact on sea birds is a metric averaging the qualitative impact on sea birds by commissioning, operation, decommissioning, area use, migration of birds, barrier effects and oil spill [55]. The evaluation is based on the known or assumed presence of chosen bird species in the areas. There was insufficient data to evaluate the impact on sea birds for Frøyabanken and Træna Vest. For these two sites, we used the qualitative values of the closest sites with available data in this study. For Frøyabanken, the impact on sea birds at Nordøyen - Ytre Vikan and Stadthavet was averaged. For Træna Vest, the same impact as at Trænafjorden was assumed.

11) Impact on fish

The impact on fish is a qualitative metrics rating the highest impact that the wind farm may have on a single fish species [55]. If the wind farm area overlaps with the spawning grounds of several fish species that will be affected, the highest reported impact is used.

12) Impact on fisheries

The impact on fisheries used here [55] is based on the evaluation by the Norwegian Directorate of Fisheries [58] which considers three factors: (i) the primary sales value, (ii) the number of vessels under 15 m, and (iii) an expert evaluation of the general value for fisheries. The sum of these factors is used as impact metrics on fisheries.

13) Community/local acceptance

Community or local acceptance is a criterion aiming to measure the support by the local community. Typical major concerns regarding wind farms are the visual and audible impact. Due to the plain landscape, offshore wind turbines can be visible at a distance of up to 20 km [59]. Emitted noise can be perceived as disturbing by local residents but is not expected to travel that far. Recreational activities such as sailing can also be affected by an OWF permitting only commercial vessels to enter the surrounding area.

14) High-level governmental support

High-level governmental support is a qualitative criterion that measures how the government is positioned towards floating offshore wind power. The governmental support has an impact on, for example, the process of granting a concession for a new OWF, the integration of wind power in the national electricity system and the expected participation in the wholesale electricity markets.

C. Designated Decision-making Variables

We determined the values of the selected decision-making variables, C_1–C_{14}, in a hybrid approach. The reports listed in [54]–[57], [60] compiled an extensive amount of data for the possible offshore sites, including the relevant data for the majority of the selected decision-making variables. However, there was missing, incomplete, ambiguous and even contradictory information for the sites discussed, such as turbine hub height (HH), turbine type, wind speed and net capacity factor. Also, the methods used when obtaining or calculating these values were not provided explicitly: It was unclear if the data was normalised for 100-m HH, if different turbine types were assumed, and so forth. In addition, the current HH of the commercial offshore wind turbines are above 100 m, i.e., as high as 140 m. Hence, estimating the average wind speed, annual energy, and capacity factor values considering wind turbines with 140-m HH will be more realistic and up-to-date. For these reasons, we chose to perform simulations to obtain the first three variables C_1–C_3 for each offshore site.

1) Simulation Model for the Wind Power Output

We used the *Renewables.ninja* [61] tool to simulate the wind power output and the capacity factor at a chosen coordinate and year based on the historic data and the chosen turbine model (capacity and hub height) using MERRA-2 (global) dataset. The simulated results were exported in the csv format with the following information: local date & time, power output, and wind speed in one-hour resolution. Table I shows the selected parameters for all sites studied in this work and the values of the calculated variables are presented in Table II.

TABLE I
SELECTED PARAMETERS FOR THE SIMULATION STUDY

Parameter	Value
Array size	10×10
Turbine spacing n	10 D
Array efficiency η_a	90.14%
Electrical efficiency η_e	98%
Turbine capacity	9500 kW
Hub height	140 m
Turbine model	Vestas V164 9500

The simulation tool incorporated the turbine efficiency, η_t, when calculating the estimated power output, P_o, based on the predetermined HH and turbine model. Then, array and electrical losses were reflected on P_o based on the efficiency values (η_a and η_e) given in Table I.

We performed an extensive literature search for the CAPEX (C_8) and OPEX (C_9) variables. Fig. 9 presents the representative CAPEX and OPEX values found in literature [18], [62]–[68]. We used box plots to summarise the variation of the values where each box indicates the 25th (bottom) and 75th percentiles (top), respectively. The central red line and the blue x marker show the median and mean, respectively. The whiskers represent the minimum and maximum values found in the literature. The corresponding references for the retrieved values are included in the figure. The CAPEX values span the range of 2.4–5 M€/MW whereas OPEX values cover 0.038–0.088 M€/MW/yr (both converted to M€for convenience). The main cost articles are determined based on the types of turbines, foundation types, platforms, moorings and anchors, the electrical grid and connections to shore, and installation. Therefore, the subject matter experts (SMEs)[1], who participated in the survey, executed within the scope of this study, evaluated the impact of these aspects on C_8 and C_9 for each site based on their professional judgement.

The rest of the variables C_4–C_7 and C_{10}–C_{14} were retrieved from the reports [54]–[57], [60]. Table II presents the designated variables for the four offshore sites where *Simulation* tab provides the calculated variables using *Renewables.ninja* and *Reported* tab depicts the retrieved data for the shown variables.

The investigations for C_{10}–C_{12} were evaluated in a Likert scale which was already compatible with the proposed fuzzy algorithm. Therefore, reported C_{10}–C_{12} were transformed into a compatible Likert scale for the model accordingly. Similarly, SMEs evaluated the impacts of C_{13} and C_{14} depending on their engineering judgement and their long-term observation of societal and energy political landscape.

In the next section, we introduce our proposed decision-making model to choose the best alternative OWF site among the four alternative locations and rank them using the designated decision-making variables in this section.

[1]The proposed decision-making procedure includes seasoned researchers with more than 10 years experience in the field of wind energy in academia and industry.

TABLE II
DESIGNATED DECISION-MAKING VARIABLES FOR THE FOUR SITES STUDIED IN THIS WORK (DATA IN PARENTHESES PROVIDE THE SPECIFIED ADDITIONAL INFORMATION)

	Simulation			Reported [54]–[57], [60]			
	C_1	C_2	C_3	C_4	C_5 & C_6	C_7	C_{10}, C_{11} & C_{12}
Location	Wind speed [m/s]†	Annual energy production [GWh/yr]	Simulated capacity factor (net CF) [%]‡	Water depth average min, max) [m]	Distance to the nearest grid (coast) [km]	Average wave height [m]	Impact on birds, fishes, fisheries*
Utsira Nord	9.99	4439	53.30 (47.08)	267 (185,280)	45 (22)	2.2	1, 1, 1
Stadthavet	10.46	4578	55.01 (48.59)	208 (168,264)	115 (58)	2.8	2, 4, 4
Frøyabanken	9.37	3835	46.10 (40.72)	210 (160,314)	83 (34)	2.5	3, 2, 2
Træna Vest	9.23	3801	45.70 (40.37)	271 (181,352)	134 (45)	2.4	4, 1, 4

† Average wind speed simulated at 140 m.
‡ Resulting net capacity factor after array and electrical losses.
* Impact evaluated with the following Likert scale; 0: none, 1: very low, $\cdots$, 5: very high in [54]–[57], [60].

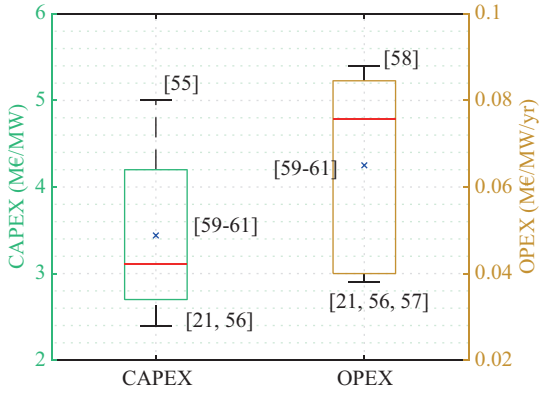

Fig. 9. Variation of the reported CAPEX (C_8) and OPEX (C_9) values in the literature [18], [62]–[68]. On each box, the central red line indicates the median, and the bottom and top edges of the box indicate the 25th and 75th percentiles, respectively, while the whiskers extend to the most extreme data points [69].

IV. PROPOSED RESEARCH MODEL

A. Preliminaries

In this section, we introduce some fundamental definitions of q-ROFSs.

Definition 1. A q-ROFS $\breve{Z}$ in a finite universe discourse $V = v_1, v_2, \cdots, v_n$ is described by Yager [40]:

$$\breve{Z} = \left\{ \left\langle v, \sigma_{\breve{Z}}(v), \varsigma_{\breve{Z}}(v) \right\rangle \middle| \, v \in V \right\} \tag{4}$$

where $\sigma_{\breve{Z}} : V \to [0,1]$ represents the degree of membership and $\varsigma_{\breve{Z}} : V \to [0,1]$ represents the degree of non-membership of the element $v \in V$ to the set $\breve{Z}$, respectively, with the condition that $0 \leq \sigma_{\breve{Z}}(v)^q + \varsigma_{\breve{Z}}(v)^q \leq 1$, where $q \geq 1$.

The degree of hesitancy is expressed as:

$$\tau_{\breve{Z}}(v) = \sqrt[q]{1 - \sigma_{\breve{Z}}(v)^q - \varsigma_{\breve{Z}}(v)^q} \tag{5}$$

For convenience, we call a $\left\langle \sigma_{\breve{Z}}(v), \varsigma_{\breve{Z}}(v) \right\rangle$ q-rung orthopair fuzzy number (q-ROFN) and characterized by $\breve{Z} = \left\langle \sigma_{\breve{Z}}, \varsigma_{\breve{Z}} \right\rangle$.

Definition 2. Let $\breve{Z} = (\sigma_{\breve{Z}}, \varsigma_{\breve{Z}})$, $\breve{Z}_1 = (\sigma_{\breve{Z}_1}, \varsigma_{\breve{Z}_1})$, and $\breve{Z}_2 = (\sigma_{\breve{Z}_2}, \varsigma_{\breve{Z}_2})$ be three q-ROFNs. After that, their operations can be expressed by Liu and Wang [70]:

$$\breve{Z}^p = \left(\sigma_{\breve{Z}}, \varsigma_{\breve{Z}}\right) \tag{6}$$

$$\breve{Z}_1 \cap \breve{Z}_2 = \left\langle \min\left\{\sigma_{\breve{Z}_1}, \sigma_{\breve{Z}_2}\right\}, \max\left\{\varsigma_{\breve{Z}_2}, \varsigma_{\breve{Z}_2}\right\} \right\rangle \tag{7}$$

$$\breve{Z}_1 \cup \breve{Z}_2 = \left\langle \max\left\{\sigma_{\breve{Z}_1}, \sigma_{\breve{Z}_1}\right\}, \min\left\{\varsigma_{\breve{Z}_2}, \varsigma_{\breve{Z}_2}\right\} \right\rangle \tag{8}$$

$$\breve{Z}_1 \oplus \breve{Z}_2 = \left\langle \sqrt[q]{\sigma_{\breve{Z}_1}^q + \sigma_{\breve{Z}_2}^q - \sigma_{\breve{Z}_1}^q \sigma_{\breve{Z}_2}^q}, \varsigma_{\breve{Z}_1} \varsigma_{\breve{Z}_2} \right\rangle \tag{9}$$

$$\breve{Z}_1 \otimes \breve{Z}_2 = \left\langle \sigma_{\breve{Z}_1} \sigma_{\breve{Z}_2}, \sqrt[q]{\varsigma_{\breve{Z}_1}^q + \varsigma_{\breve{Z}_2}^q - \varsigma_{\breve{Z}_1}^q \varsigma_{\breve{Z}_2}^q} \right\rangle \tag{10}$$

$$\lambda\breve{Z} = \left\langle \left(\sqrt[q]{1 - (1 - \sigma_{\breve{Z}}^q)^\lambda}, \varsigma_{\breve{Z}}^\lambda \right) \right\rangle \tag{11}$$

$$\breve{Z}^\lambda = \left\langle \left(\sigma_{\breve{Z}}^\lambda, \sqrt[q]{1 - (1 - \varsigma_{\breve{Z}}^q)^\lambda} \right) \right\rangle \tag{12}$$

where $\lambda > 0$, and p is the complementary set of $\breve{Z}$.

Definition 3. A Let $\breve{Z} = \left(\sigma_{\breve{Z}}, \varsigma_{\breve{Z}}\right)$ be a q-ROFN, the score function $S(\breve{Z})$ of $\breve{Z}$ can be expressed by Wei *et al.* [71]:

$$S(\breve{Z}) = \frac{1}{2}\left(1 + \sigma_{\breve{Z}}^q - \varsigma_{\breve{Z}}^q\right) \tag{13}$$

Peng and Dai [72] defined the score function differently:

$$S_\lambda(\breve{Z}) = \frac{1}{3}\left(\sigma_{\breve{Z}}^q - 2\varsigma_{\breve{Z}}^q - 1\right) + \frac{\lambda}{3}\left(\sigma_{\breve{Z}}^q + \varsigma_{\breve{Z}}^q + 2\right) \tag{14}$$

Definition 4. A Let $\breve{Z} = \left(\sigma_{\breve{Z}}, \varsigma_{\breve{Z}}\right)$ be a q-ROFN, the accuracy function $A(\breve{Z})$ of $\breve{Z}$ can be expressed by Liu and Wang [70]:

$$A(\breve{Z}) = \sigma_{\breve{Z}}^q + \varsigma_{\breve{Z}}^q \tag{15}$$

Definition 5. Let $\breve{Z}_i = (\sigma_{\breve{Z}_i}, \varsigma_{\breve{Z}_i})$ $(i = 1, 2, \cdots, n)$ be set of q-ROFNs and $w = (w_1, w_2, \cdots, w_n)^{\mathrm{T}}$ be weight vector of $\breve{Z}_i$ with $\sum_{i=1}^n w_i = 1$ and $w_i \in [0,1]$. q-rung orthopair fuzzy weighted average (q-ROFWA) and q-rung orthopair fuzzy weighted geometric (q-ROFWG) operators can be expressed by Liu and Wang [70], respectively:

$$\text{q-ROFWA}\left(\breve{Z}_1, \breve{Z}_2, \cdots, \breve{Z}_n\right) = \left(\left(1 - \prod_{i=1}^n \left(1 - \sigma_{\breve{Z}_i}^q\right)^{w_i}\right)^{\frac{1}{q}}, \prod_{i=1}^n \varsigma_{\breve{Z}_i}^{w_i} \right) \tag{16}$$

$$\text{q-ROFWG}\left(\breve{Z}_1, \breve{Z}_2, \cdots, \breve{Z}_n\right) = \left(\prod_{i=1}^n \sigma_{\breve{Z}_i}^{w_i}, \left(1 - \prod_{i=1}^n \left(1 - \varsigma_{\breve{Z}_i}^q\right)^{w_i}\right)^{\frac{1}{q}} \right) \tag{17}$$

B. Weighted q-rung orthopair fuzzy Hamacher average operator

Definition 6. Let $\breve{Z}_i = \left(\sigma_{\breve{Z}_i}, \varsigma_{\breve{Z}_i}\right)$ $(i = 1, 2, \cdots, n)$ be set of q-ROFNs and $w = (w_1, w_2, \cdots, w_n)^{\mathrm{T}}$ be weight vector of

$\breve{Z}_i$ with $\sum_{i=1}^{n} w_i = 1$ and $w_i \in [0,1]$. The weighted q-rung orthopair fuzzy Hamacher average (Wq-ROFHA) operator is defined by Darko and Liang [73]:

$$\text{Wq-ROFHA}\left(\breve{Z}_1, \breve{Z}_2, \cdots, \breve{Z}_n\right) = w_1(\breve{Z}_1) \oplus w_2(\breve{Z}_2) \oplus \cdots \oplus w_n(\breve{Z}_n) = \oplus_{i=1}^{n} w_i(\breve{Z}_i) \quad (18)$$

$$\text{Wq-ROFHA}\left(\breve{Z}_1, \breve{Z}_2, \cdots, \breve{Z}_n\right) = \left(\sqrt[q]{\frac{\prod_{i=1}^{n}\left(1+(\gamma-1)(\sigma_{\breve{Z}_i})^q\right)^{w_i} - \prod_{i=1}^{n}\left(1-(\sigma_{\breve{Z}_i})^q\right)^{w_i}}{\prod_{i=1}^{n}\left(1+(\gamma-1)(\sigma_{\breve{Z}_i})^q\right)^{w_i} + (\gamma-1)\prod_{i=1}^{n}\left(1-(\sigma_{\breve{Z}_i})^q\right)^{w_i}}}, \frac{\sqrt[q]{\gamma}\prod_{i=1}^{n}(\varsigma_{\breve{Z}_i})^{w_i}}{\sqrt[q]{\prod_{i=1}^{n}\left(1+(\gamma-1)(1-(\varsigma_{\breve{Z}_i})^q)\right)^{w_i} + (\gamma-1)\prod_{i=1}^{n}(\varsigma_{\breve{Z}_i})^{qw_i}}} \right) \quad (19)$$

where $\gamma > 0$ and $q \geq 0$.

C. Weighted q-rung orthopair fuzzy Hamacher geometric mean operator

Definition 7. Let $\breve{Z}_i = (\sigma_{\breve{Z}_i}, \varsigma_{\breve{Z}_i})$ $(i = 1, 2, \cdots, n)$ be set of q-ROFNs and $w = (w_1, w_2, \cdots, w_n)^{\mathrm{T}}$ be weight vector of $\breve{Z}_i$ with $\sum_{i=1}^{n} w_i = 1$ and $w_i \in [0,1]$. The weighted q-rung orthopair fuzzy Hamacher geometric mean (Wq-ROFHGM) operator is defined by Darko and Liang [73]:

$$\text{Wq-ROFHGM}\left(\breve{Z}_1, \breve{Z}_2, \cdots, \breve{Z}_n\right) = \left(\frac{\sqrt[q]{\gamma}\prod_{i=1}^{n}(\sigma_{\breve{Z}_i})^{w_i}}{\prod_{i=1}^{n}\left(1+(\gamma-1)(1-(\sigma_{\breve{Z}_i})^q)\right)^{w_i} + (\gamma-1)\prod_{i=1}^{n}\left(\sigma_{\breve{Z}_i}\right)^{qw_i}}, \sqrt[q]{\frac{\prod_{i=1}^{n}\left(1+(\gamma-1)(\varsigma_{\breve{Z}_i})^q\right)^{w_i} - \prod_{i=1}^{n}\left(1-(\varsigma_{\breve{Z}_i})^q\right)^{w_i}}{\prod_{i=1}^{n}\left(1+(\gamma-1)(\varsigma_{\breve{Z}_i})^q\right)^{w_i} + (\gamma-1)\prod_{i=1}^{n}\left(1-(\varsigma_{\breve{Z}_i})^q\right)^{w_i}}} \right) \quad (20)$$

where $\gamma > 0$ and $q \geq 0$.

D. Proposed Model

In this section, we introduce an integrated decision-making model. Firstly, to determine the criteria weights, q-ROFSs based FUCOM is proposed. Later, the CoCoSo approach, which is proposed by Yazdani *et al*. [74] into the q-ROFSs environment including Wq-ROFHA and Wq-ROFHGM to choose the best alternative OWF site among four alternatives and rank them. The flowchart of the proposed model is shown in Fig. 10.

Step 1: In terms of the proposed model, we determine the site selection criteria, and define the alternative offshore wind farm areas, and form the committee experts. We identify the set of alternatives $A_j = A_1, A_2, \cdots, A_m$ $(j = 1, 2, , m)$, and the set of the criteria $C_i = C_1, C_2, \cdots, C_n$ $(i = 1, 2, , n)$ is assessed by h experts of set $E = E_1, E_2, \cdots, E_h$ $(e = 1, 2, , h)$.

Step 2: Select the linguistic terms and determine their corresponding values for evaluating criteria and alternatives.

Step 3: Calculate the criteria weights using the q-ROF based FUCOM methodology.

Determining the weight coefficients of the criteria is a crucial phase in applying multi-criteria models and defining the

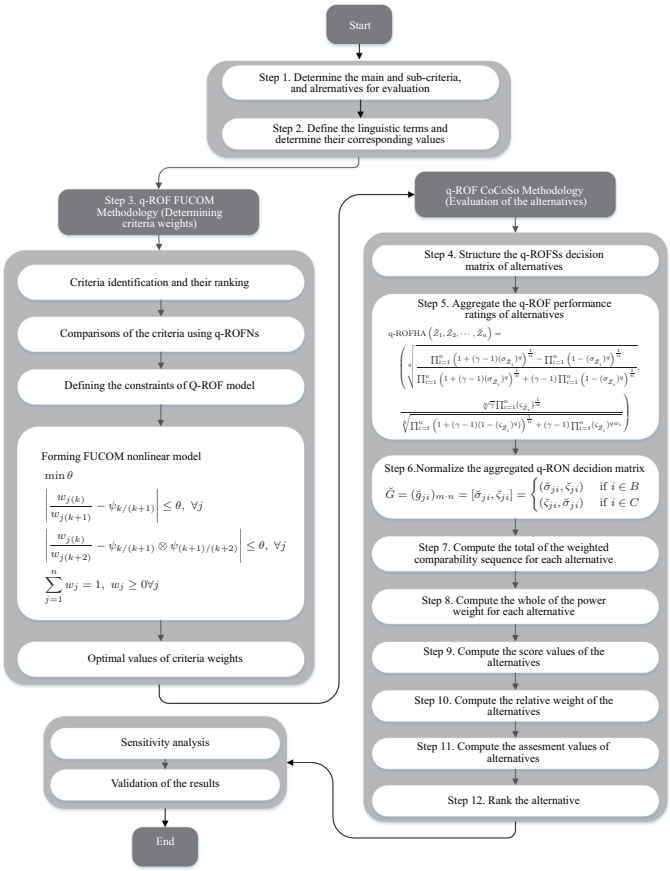

Fig. 10. q-ROFSs based FUCOM and fuzzy Hamacher based CoCoSo model.

aggregated criterion functions of the alternatives. To objectify the entire decision-making process using the q-ROF CoCoSo methodology, the following section presents a novel q-ROF FUCOM (Full Consistency Method) method. The q-ROF FUCOM method was developed based on the conventional FUCOM developed by Pamucar *et al*. [75]. This method provides the possibility of objective and rational determination of the weight coefficients of the criteria with a minimum number of comparisons and maximum satisfaction of the consistency of the comparison. In the following section, the q-ROF FUCOM method is presented through the steps:

Step 3.1: The initial phase of the q-ROF FUCOM method involves the individual definition of significance and ranking of criteria by experts e_h $(h = 1, 2, \cdots, b)$. Thus we get the rank of the criterion $C^h_{j(1)} > C^h_{j(2)} > \cdots > C^h_{j(k)}$ $(j = 1, 2, \cdots, n)$, where $C_{x(k-1)} > C_{y(k)}$ $(C_x, C_y \in C_j, j = 1, 2, \cdots, n)$ means that the criterion has a greater significance than the criterion C_y, since $(k-1) > k$.

Step 3.2: After defining the ranks of the criteria, the experts compare the criteria in pairs. Comparison of criteria is represented by a vector of comparative significance according to (21):

$$\Phi^h = \begin{matrix} C_{j1} & C_{j2} & \cdots & C_{jk} \end{matrix} \quad (21)$$
$$\begin{pmatrix} \varpi^h_{C_{j(1)}} = (\sigma^h_{Z_1}, \varsigma^h_{Z_1}) & \varpi^h_{C_{j(2)}} = (\sigma^h_{Z_2}, \varsigma^h_{Z_2}) & \cdots & \varpi^h_{C_{j(k)}} = (\sigma^h_{Z_k}, \varsigma^h_{Z_k}) \end{pmatrix}$$

where Φ^h represents the individual experts' vector of compar-

ative significance.

The criteria were compared using the fuzzy preference scale shown in Table III.

TABLE III
FUZZY PREFERENCE SCALE [76]

Preference on pairwise comparison	Fuzzy preference number
Extremely not preferred	0.1
Very strongly not preferred	0.2
Strongly not preferred	0.3
Moderately not preferred	0.4
Equally preferred	0.5
Moderately preferred	0.6
Strongly preferred	0.7
Very strongly preferred	0.8
Extremely preferred	0.9
Intermediate values	Other values between 0.1 and 0.9

Step 3.3: Defining the constraints of a nonlinear q-ROF FUCOM model. The first group of constraints is defined based on vectors of comparative significance (see (21)). The weighting coefficients should meet the condition that $w_k^h/w_{k+1}^h = \psi_{k/(k+1)}^h$, where $\psi_{k/(k+1)}^h = \varpi_{C_{j(k+1)}}^h/\varpi_{C_{j(k)}}^h$ represents the significance that the rank criterion has in relation to the criterion $C_{j(k+1)}$.

The second group of constraints is defined based on the conditions of transitivity between the comparative meanings of the criteria. The transitivity between the significance of the criteria is defined by the condition that $\psi_{k/(k+1)} \otimes \psi_{(k+1)/(k+2)} = \psi_{k/(k+2)}$, i.e., $w_k \otimes w_{k+1/k+2} = w_{k/k+2}$.

Based on the defined constraints, we can present the q-ROF FUCOM model to calculate the optimal values of the criteria as in (22):

$$\begin{aligned} &\min \theta \\ &\text{s.t.} \quad \left|\frac{w_{j(k)}}{w_{j(k+1)}} - \psi_{k/(k+1)}\right| \le 0, \forall_j \\ &\qquad \left|\frac{w_{j(k)}}{w_{j(k+2)}} - \psi_{k/(k+1)} \otimes \psi_{(k+1)/(k+2)}\right| \le 0, \forall_j \\ &\qquad \sum_{j=1}^{n} w_j = 1, w_j \ge 0, \forall_j \end{aligned} \tag{22}$$

By solving model (see (22)), we obtain a vector of weight coefficients $(w_1, w_2, \cdots, w_n)^{\mathrm{T}}$.

Step 4: Build the decision matrices $\breve{\boldsymbol{F}}_h = (\breve{f}_{jih})_{m\cdot n} = [\breve{\sigma}_{jih}, \breve{\varsigma}_{jih}]$ based on q-ROFSs in terms of experts' opinion with the help of Table IV. Alternatives for each criterion are evaluated by Experts (E_h) using the q-ROFSs in Table IV.

$$\breve{\boldsymbol{F}} = \left(\breve{f}_{jih}\right)_{m\cdot n} = \begin{array}{c} \\ C_1 \\ C_2 \\ \vdots \\ C_n \end{array} \begin{array}{c} \begin{array}{cccc} A_1 & A_2 & \cdots & A_m \end{array} \\ \begin{pmatrix} \langle(\breve{\sigma}_{11h}, \breve{\varsigma}_{11h})\rangle & \langle(\breve{\sigma}_{12h}, \breve{\varsigma}_{12h})\rangle & \cdots & \langle(\breve{\sigma}_{1mh}, \breve{\varsigma}_{1mh})\rangle \\ \langle(\breve{\sigma}_{21h}, \breve{\varsigma}_{21h})\rangle & \langle(\breve{\sigma}_{22h}, \breve{\varsigma}_{22h})\rangle & \cdots & \langle(\breve{\sigma}_{2mh}, \breve{\varsigma}_{2mh})\rangle \\ \vdots & \vdots & \ddots & \vdots \\ \langle(\breve{\sigma}_{n1h}, \breve{\varsigma}_{n1h})\rangle & \langle(\breve{\sigma}_{n2h}, \breve{\varsigma}_{n2h})\rangle & \cdots & \langle(\breve{\sigma}_{nmh}, \breve{\varsigma}_{nmh})\rangle \end{pmatrix} \end{array} \tag{23}$$

TABLE IV
LINGUISTIC TERMS FOR EVALUATIONS OF EACH ALTERNATIVE [42]

Linguistic terms	q-ROFN for alternatives	
	σ	ς
Extremely low (EL)	0.15	0.95
Very low (VL)	0.25	0.85
Low (L)	0.35	0.75
Medium low (ML)	0.45	0.65
Medium (M)	0.55	0.55
Medium high (MH)	0.65	0.45
High (H)	0.75	0.35
Very high (VH)	0.85	0.25
Extremely high (EH)	0.95	0.15

where m and n denote the number of alternatives and criteria, respectively. $\breve{f}_{jih} = [\breve{\sigma}_{jih}, \breve{\varsigma}_{jih}]$ represents the performance of alternative A_j with respect to criterion C_j of hth expert.

Step 5: Aggregate the q-ROF performance ratings of alternatives regarding each expert and form the q-ROF decision matrix $(\breve{\boldsymbol{F}})$. The individual decision matrices are aggregated with the help of (24) and the q-rung orthopair fuzzy weighted averaging (q-ROFWA) operator given in (16).

$$\breve{\boldsymbol{F}} = \left(\breve{f}_{ji}\right)_{m\cdot n} = \begin{array}{c} \\ C_1 \\ C_2 \\ \vdots \\ C_n \end{array} \begin{array}{c} \begin{array}{cccc} A_1 & A_2 & \cdots & A_m \end{array} \\ \begin{pmatrix} \langle(\breve{\sigma}_{11}, \breve{\varsigma}_{11})\rangle & \langle(\breve{\sigma}_{12h}, \breve{\varsigma}_{12})\rangle & \cdots & \langle(\breve{\sigma}_{1m}, \breve{\varsigma}_{1m})\rangle \\ \langle(\breve{\sigma}_{21}, \breve{\varsigma}_{21})\rangle & \langle(\breve{\sigma}_{22}, \breve{\varsigma}_{22})\rangle & \cdots & \langle(\breve{\sigma}_{2m}, \breve{\varsigma}_{2m})\rangle \\ \vdots & \vdots & \ddots & \vdots \\ \langle(\breve{\sigma}_{n1}, \breve{\varsigma}_{n1})\rangle & \langle(\breve{\sigma}_{n2}, \breve{\varsigma}_{n2})\rangle & \cdots & \langle(\breve{\sigma}_{nm}, \breve{\varsigma}_{nm})\rangle \end{pmatrix} \end{array} \tag{24}$$

$\breve{f}_{ji} = [\breve{\sigma}_{ji}, \breve{\varsigma}_{ji}]$ represents the aggregated q-ROFN of jth alternative in terms of ith criterion.

Step 6: Normalise the aggregated q-RON decision matrix $(\breve{\boldsymbol{G}})$ according to (25):

$$\breve{\boldsymbol{G}} = (\breve{g}_{ji})_{m\cdot n} = [\breve{\sigma}_{ji}, \breve{\varsigma}_{ji}] = \begin{cases} (\breve{\sigma}_{ji}, \breve{\varsigma}_{ji}) & \text{if } i \in B \\ (\breve{\varsigma}_{ji}, \breve{\sigma}_{ji}) & \text{if } i \in C \end{cases} \tag{25}$$

where B and C indicate the set of benefit and cost criteria, respectively.

After that, the CoCoSo approach is implemented to the model. The steps of this approach are as follows [74]:

Step 7: Compute the total of the weighted comparability sequence (α_j) for each alternative using Wq-ROFHA given in (18) and (19).

Step 8: Compute the whole of the power weight (β_j) of comparability sequences for each alternative using the weighted q-rung orthopair fuzzy Hamacher geometric mean (Wq-ROFHGM) operator given in (20).

Step 9: Compute the score values of the alternatives using the values of Wq-ROFHA and Wq-ROFHGM for each alternative with the help of (13).

Step 10: Compute the relative weight of the alternatives using (26)–(28).

$$X_{ja} = \frac{\alpha_j + \beta_j}{\sum_{j=1}^{m}(\alpha_j + \beta_j)} \tag{26}$$

$$X_{jb} = \frac{\alpha_j}{\min(\alpha_j)} + \frac{\beta_j}{\min(\beta_j)} \tag{27}$$

$$X_{jc} = \frac{\psi\alpha_j + (1-\psi)\beta_j}{\psi\max(\alpha_j) + (1-\psi)\max(\beta_j)},\ 0 \le \psi \le 1 \tag{28}$$

where X_{ja}, X_{jb}, and X_{jc} represent the aggregation score strategies as follows: (i) X_{ja} is the arithmetic mean of sums of weighted sum method (WSM) and weighted product model (WPM) scores, (ii) X_{jb} is the sum of relative scores of WSM and WPM, (iii) X_{jc} is the balanced compromise of WSM and WPM models scores.

Step 11: Compute the assessment values (X_j) of the alternatives using (29).

$$X_j = \sqrt[3]{X_{ja}X_{jb}X_{jc}} + \frac{X_{ja} + X_{jb} + X_{jc}}{3} \tag{29}$$

Step 12: Rank the alternative according to the decreasing value of X_j.

V. Experimental Results and Discussion

In this section, the results of the application of the proposed hybrid model are presented.

Step 1: A set of four experts participated in the survey to evaluate four different OWF sites. These experts assess the performance of four alternative sites in terms of two main and fourteen criteria.

Step 2: Identified linguistic terms for evaluation of alternatives are presented in Table IV.

Step 3: In this step, the calculation of criterion weights is presented.

Steps 3.1 and 3.2: In the first step, it is necessary to define the significance and rank of the criteria on the previously defined q-ROF FUCOM algorithm. Since four experts participated in this research, each expert defined their importance separately within each cluster, as shown in Table V.

Step 3.3: Based on the expert assessments from Table V, the constraints used to solve the q-ROF FUCOM model (22) are defined. By applying (13), we obtain score values based on which significant values are specified in Table VI.

Based on the vector of comparative significance (Tables V and VI), we can define model constraints (22). Then, a nonlinear model is defined for each level of criteria, based on which the local weight coefficients of the criteria are obtained. Since four experts participate in the research, 12 models are formed, i.e., three models for each expert. The following section presents the procedure for developing a nonlinear q-ROF FUCOM model for the first expert and a group of techno-economic (MC_1) criteria.

Based on the score values (see Table VI) we can define the first group of constraints according to the following:

$$\psi^1_{C_3/C_2} = \varphi_{C_3}/\varphi_{C_2} = 0.600/0.500 = 1.20;$$
$$\psi^1_{C_2/C_1} = \varphi_{C_2}/\varphi_{C_1} = 0.625/0.600 = 1.04;$$
$$\psi^1_{C_1/C_8} = \varphi_{C_1}/\varphi_{C_8} = 0.725/0.625 = 1.16;$$
$$\psi^1_{C_2/C_1} = \varphi_{C_2}/\varphi_{C_1} = 0.775/0.725 = 1.07;$$
$$\psi^1_{C_9/C_4} = \varphi_{C_4}/\varphi_{C_9} = 0.825/0.775 = 1.06;$$
$$\psi^1_{C_4/C_5} = \varphi_{C_5}/\varphi_{C_4} = 0.890/0.825 = 1.08;$$
$$\psi^1_{C_5/C_6} = \varphi_{C_6}/\varphi_{C_5} = 0.925/0.890 = 1.04;$$
$$\psi^1_{C_6/C_7} = \varphi_{C_7}/\varphi_{C_6} = 0.975/0.925 = 1.05.$$

The second group of constraints is defined based on the conditions of transitivity between the comparative meanings of the criteria:

$$\psi^1_{C_3/C_1} = 1.20 \cdot 1.04 = 1.25;$$
$$\psi^1_{C_2/C_8} = 1.04 \cdot 1.16 = 1.21;$$
$$\psi^1_{C_1/C_9} = 1.16 \cdot 1.07 = 1.24;$$
$$\psi^1_{C_8/C_4} = 1.07 \cdot 1.06 = 1.14;$$
$$\psi^1_{C_9/C_5} = 1.06 \cdot 1.08 = 1.15;$$
$$\psi^1_{C_4/C_6} = 1.08 \cdot 1.04 = 1.12;$$
$$\psi^1_{C_5/C_7} = 1.04 \cdot 1.05 = 1.10.$$

TABLE V
Evaluations of Criteria/sub-criteria

Rank	Expert 1		Expert 2		Expert 3		Expert 4	
	Criteria	q-ROF	Criteria	q-ROF	Criteria	q-ROF	Criteria	q-ROF
Main criteria								
1	MC_1	(0.50, 0.50)	MC_1	(0.50, 0.50)	MC_1	(0.50, 0.50)	MC_1	(0.50, 0.50)
2	MC_2	(0.90, 0.00)	MC_2	(0.55, 0.45)	MC_2	(0.80, 0.18)	MC_2	(0.60, 0.45)
Techno-economical (MC_1)								
1	C_3	(0.50, 0.50)	C_2	(0.50, 0.50)	C_3	(0.50, 0.50)	C_2	(0.50, 0.50)
2	C_2	(0.55, 0.35)	C_1	(0.60, 0.35)	C_2	(0.55, 0.45)	C_8	(0.60, 0.45)
3	C_1	(0.60, 0.35)	C_3	(0.65, 0.30)	C_1	(0.60, 0.35)	C_9	(0.65, 0.35)
4	C_8	(0.70, 0.25)	C_8	(0.75, 0.25)	C_8	(0.65, 0.30)	C_1	(0.70, 0.30)
5	C_9	(0.75, 0.20)	C_9	(0.75, 0.25)	C_9	(0.75, 0.25)	C_3	(0.75, 0.25)
6	C_4	(0.80, 0.15)	C_4	(0.85, 0.20)	C_5	(0.80, 0.20)	C_5	(0.85, 0.20)
7	C_5	(0.88, 0.10)	C_5	(0.90, 0.10)	C_6	(0.85, 0.15)	C_6	(0.85, 0.20)
8	C_6	(0.90, 0.05)	C_6	(0.95, 0.00)	C_7	(0.90, 0.10)	C_4	(0.90, 0.10)
9	C_7	(0.95, 0.00)	C_7	(0.95, 0.00)	C_4	(0.95, 0.05)	C_7	(0.95, 0.05)
Environmental and Social (MC_2)								
1	C_{14}	(0.50, 0.50)	C_{14}	(0.50, 0.50)	C_{14}	(0.50, 0.50)	C_{14}	(0.50, 0.50)
2	C_{12}	(0.60, 0.45)	C_{11}	(0.60, 0.45)	C_{13}	(0.70, 0.25)	C_{13}	(0.65, 0.35)
3	C_{11}	(0.70, 0.30)	C_{12}	(0.70, 0.30)	C_{10}	(0.85, 0.15)	C_{12}	(0.70, 0.30)
4	C_{10}	(0.80, 0.20)	C_{10}	(0.80, 0.20)	C_{11}	(0.90, 0.05)	C_{10}	(0.85, 0.20)
5	C_{13}	(0.90, 0.00)	C_{13}	(0.90, 0.00)	C_{12}	(0.95, 0.00)	C_{11}	(0.95, 0.00)

TABLE VI
SCORE VALUES OF CRITERIA/SUB-CRITERIA

Rank	Expert 1		Expert 2		Expert 3		Expert 4	
	Criteria	Score value	Criteria	Score value	Criteria	Score value	Criteria	Score value
Main criteria								
1	MC_1	0.500	MC_1	0.500	MC_1	0.500	MC_1	0.500
2	MC_2	0.950	MC_2	0.550	MC_2	0.810	MC_2	0.575
Techno-economical (MC_1)								
1	C_3	0.500	C_2	0.500	C_3	0.500	C_2	0.500
2	C_2	0.600	C_1	0.625	C_2	0.550	C_8	0.575
3	C_1	0.625	C_3	0.675	C_1	0.625	C_9	0.650
4	C_8	0.725	C_8	0.750	C_8	0.675	C_1	0.700
5	C_9	0.775	C_9	0.750	C_9	0.750	C_3	0.750
6	C_4	0.825	C_4	0.825	C_5	0.800	C_5	0.825
7	C_5	0.890	C_5	0.900	C_6	0.850	C_6	0.825
8	C_6	0.925	C_6	0.975	C_7	0.900	C_4	0.900
9	C_7	0.975	C_7	0.975	C_4	0.950	C_7	0.950
Environmental and Social (MC_2)								
1	C_{14}	0.500	C_{14}	0.500	C_{14}	0.500	C_{14}	0.500
2	C_{12}	0.575	C_{11}	0.575	C_{13}	0.725	C_{13}	0.650
3	C_{11}	0.700	C_{12}	0.700	C_{10}	0.850	C_{12}	0.700
4	C_{10}	0.800	C_{10}	0.800	C_{11}	0.925	C_{10}	0.825
5	C_{13}	0.950	C_{13}	0.950	C_{12}	0.975	C_{11}	0.975

Based on the presented constraints, the q-ROF FUCOM model is defined for the group of techno-economical (MC_1) criteria as follows:

$$\text{Expert 1: } \min \theta$$

s.t.

$$\left|\frac{w_3}{w_2} - 1.2\right| \le \theta; \left|\frac{w_2}{w_1} - 1.04\right| \le \theta; \cdots; \left|\frac{w_8}{w_9} - 1.07\right| \le \theta;$$
$$\left|\frac{w_9}{w_4} - 1.06\right| \le \theta; \left|\frac{w_4}{w_5} - 1.08\right| \le \theta; \cdots; \left|\frac{w_6}{w_7} - 1.05\right| \le \theta;$$
$$\left|\frac{w_3}{w_1} - 1.25\right| \le \theta; \left|\frac{w_2}{w_8} - 1.21\right| \le \theta; \cdots; \left|\frac{w_8}{w_4} - 1.14\right| \le \theta;$$
$$\left|\frac{w_9}{w_5} - 1.15\right| \le \theta; \left|\frac{w_4}{w_6} - 1.12\right| \le \theta; \left|\frac{w_5}{w_7} - 1.10\right| \le \theta;$$
$$\sum_{j=1}^{9} w_j = 1, w_j \ge 0, \forall_j$$

Models for the remaining criteria levels are defined similarly. By solving the q-ROF FUCOM model, the final values of the weight coefficients of the criteria are obtained, as presented in Table VII.

Step 4: The experts expressed their opinions, as presented in Table VIII, using the scale in Table IV with the help of (23) for four alternatives in terms of fourteen criteria. Then, the linguistic evaluations of experts are converted to the corresponding q-ROFNs in Table IV.

Step 5: The experts' evaluations are aggregated by (16) and (24). The aggregated q-ROF decision matrix is given in Table IX.

Step 6: The q-ROF normalised decision matrix is structured with the help of Table IX using (25) and is presented in Table X.

Steps 7–8: The total of the weighted (α_j) and the whole of the power weight (β_j) of comparability sequences for each alternative are constructed by Wq-ROFHA operator given in (18)–(19), and Wq-ROFHGM operator given in (20) using the normalised q-ROF values given in Table X. The values of each alternative for Wq-ROFHA and Wq-ROFHGM operators are reported in Table XI.

TABLE VII
WEIGHTING COEFFICIENTS OF THE CRITERIA

Criteria	Expert 1	Expert 2	Expert 3	Expert 4	Average	Global
MC_1	0.6391	0.52381	0.6181	0.5362	0.5793	–
C_1	0.1294	0.1319	0.1248	0.1130	0.1248	0.0723
C_2	0.1350	0.1649	0.1419	0.1586	0.1501	0.0870
C_3	0.1616	0.1225	0.1563	0.1057	0.1365	0.0791
C_4	0.0979	0.0999	0.0817	0.0881	0.0919	0.0532
C_5	0.0908	0.0914	0.0974	0.0959	0.0939	0.0544
C_6	0.0872	0.0849	0.0918	0.0959	0.0899	0.0521
C_7	0.0828	0.0843	0.0864	0.0832	0.0842	0.0488
C_8	0.1113	0.1102	0.1156	0.1379	0.1188	0.0688
C_9	0.1041	0.1100	0.1040	0.1218	0.1100	0.0637
MC_2	0.3609	0.4762	0.3819	0.4638	0.4207	–
C_{10}	0.1647	0.1675	0.1768	0.1681	0.1697	0.0712
C_{11}	0.1944	0.2330	0.1619	0.1424	0.1785	0.0770
C_{12}	0.2222	0.1911	0.1540	0.1982	0.1917	0.0805
C_{13}	0.1388	0.1406	0.2070	0.2137	0.1758	0.0736
C_{14}	0.2799	0.2677	0.3003	0.2776	0.2843	0.1184

Step 9: The score values for each alternative in terms of α_j and β_j are given in Table XII using Table XI and (13). For example, the score values of the alternative A_1 for α_j and β_j can be calculated as follows:

$$S(\alpha_{A_1}) = \frac{1}{2}(1 + 0.761 - -0.366) = 0.697,$$

and

$$S(\beta_{A_1}) = \frac{1}{2}(1 + 0.612 - -0.506) = 0.553.$$

Step 10: The relative weights X_{ja}, X_{jb} and X_{jc} of the alternatives are calculated using aggregation score strategies with the help of (26)–(28). These values are presented in Table XIII. For alternative A_1, the relative weights can be calculated as follows:

$$X_{1a} = \frac{0.697 + 0.553}{4.116} = 0.304,$$

TABLE VIII
THE PERFORMANCE RATING OF ALTERNATIVES IN TERMS OF CRITERIA

Alternatives	Experts	Criteria													
		C_1	C_2	C_3	C_4	C_5	C_6	C_7	C_8	C_9	C_{10}	C_{11}	C_{12}	C_{13}	C_{14}
A_1	E_1	VH	VH	VH	VH	MH	MH	H	H	H	VL	VL	VL	H	EH
	E_2	VH	VH	VH	H	VH	H	H	VH	VH	ML	H	H	M	H
	E_3	H	H	H	H	H	H	H	VH	VH	M	ML	ML	M	H
	E_4	H	H	H	VH	EH	H	H	EH	VH	H	VL	H	M	H
A_2	E_1	H	VH	VH	VH	L	ML	H	VH	VH	VL	VL	VL	VH	EH
	E_2	VH	VH	VH	H	H	MH	VH	VH	VH	ML	H	H	VL	H
	E_3	H	H	H	H	ML	M	H	VH	VH	M	ML	ML	M	H
	E_4	H	H	H	EH	VH	M	H	EH	VH	H	VL	H	L	H
A_3	E_1	H	VH	VH	VH	H	M	H	VH	H	VL	VL	VL	M	EH
	E_2	VH	VH	VH	H	EH	VH	VH	VH	H	ML	H	H	M	H
	E_3	H	H	H	H	VH	MH	H	VH	H	M	ML	ML	M	H
	E_4	H	H	H	VH	EH	H	H	VH	H	H	VL	H	M	H
A_4	E_1	H	VH	VH	VH	H	M	H	VH	H	VL	VL	VL	M	EH
	E_2	VH	VH	VH	H	EH	VH	VH	VH	H	ML	H	H	M	H
	E_3	H	H	H	H	VH	MH	H	VH	H	M	ML	ML	M	H
	E_4	H	H	H	VH	EH	H	H	VH	H	H	VL	H	M	H

TABLE IX
THE AGGREGATED Q-ROF DECISION MATRIX

Alternatives	C_1	C_2	C_3	C_4	C_5	C_6	C_7
A_1	[0.78, 0.322]	[0.85, 0.25]	[0.85, 0.25]	[0.85, 0.25]	[0.655, 0.451]	[0.556, 0.545]	[0.75, 0.35]
A_2	[0.85, 0.25]	[0.85, 0.25]	[0.85, 0.25]	[0.75, 0.35]	[0.902, 0.211]	[0.789, 0.315]	[0.83, 0.272]
A_3	[0.75, 0.35]	[0.75, 0.35]	[0.75, 0.35]	[0.75, 0.35]	[0.764, 0.345]	[0.657, 0.444]	[0.75, 0.35]
A_4	[0.75, 0.35]	[0.75, 0.35]	[0.75, 0.35]	[0.886, 0.22]	[0.934, 0.17]	[0.71, 0.392]	[0.75, 0.35]
Alternatives	C_8	C_9	C_{10}	C_{11}	C_{12}	C_{13}	C_{14}
A_1	[0.83, 0.272]	[0.78, 0.322]	[0.25, 0.85]	[0.25, 0.85]	[0.25, 0.85]	[0.705, 0.403]	[0.95, 0.15]
A_2	[0.85, 0.25]	[0.806, 0.296]	[0.45, 0.65]	[0.75, 0.35]	[0.75, 0.35]	[0.489, 0.613]	[0.75, 0.35]
A_3	[0.85, 0.25]	[0.806, 0.296]	[0.55, 0.55]	[0.45, 0.65]	[0.45, 0.65]	[0.55, 0.55]	[0.75, 0.35]
A_4	[0.913, 0.194]	[0.806, 0.296]	[0.75, 0.35]	[0.25, 0.85]	[0.75, 0.35]	[0.507, 0.594]	[0.75, 0.35]

TABLE X
THE NORMALISED Q-ROF DECISION MATRIX

Alternatives	C_1	C_2	C_3	C_4	C_5	C_6	C_7
A_1	[0.78, 0.322]	[0.85, 0.25]	[0.85, 0.25]	[0.25, 0.85]	[0.451, 0.655]	[0.545, 0.556]	[0.35, 0.75]
A_2	[0.85, 0.25]	[0.85, 0.25]	[0.85, 0.25]	[0.35, 0.75]	[0.211, 0.902]	[0.315, 0.789]	[0.272, 0.83]
A_3	[0.75, 0.35]	[0.75, 0.35]	[0.75, 0.35]	[0.35, 0.75]	[0.345, 0.764]	[0.444, 0.657]	[0.35, 0.75]
A_4	[0.75, 0.35]	[0.75, 0.35]	[0.75, 0.35]	[0.22, 0.886]	[0.17, 0.934]	[0.392, 0.71]	[0.35, 0.75]
Alternatives	C_8	C_9	C_{10}	C_{11}	C_{12}	C_{13}	C_{14}
A_1	[0.272, 0.83]	[0.322, 0.78]	[0.85, 0.25]	[0.85, 0.25]	[0.85, 0.25]	[0.705, 0.403]	[0.95, 0.15]
A_2	[0.25, 0.85]	[0.296, 0.806]	[0.65, 0.45]	[0.35, 0.75]	[0.35, 0.75]	[0.489, 0.613]	[0.75, 0.35]
A_3	[0.25, 0.85]	[0.296, 0.806]	[0.55, 0.55]	[0.65, 0.45]	[0.65, 0.45]	[0.55, 0.55]	[0.75, 0.35]
A_4	[0.194, 0.913]	[0.296, 0.806]	[0.35, 0.75]	[0.85, 0.25]	[0.35, 0.75]	[0.507, 0.594]	[0.75, 0.35]

TABLE XI
THE α_j AND β_j VALUES OF ALTERNATIVES

Alternatives	Wq-ROFHA Operator		Wq-ROFHGM Operator	
	α	β	α	β
A_1	0.761	0.366	0.612	0.506
A_2	0.604	0.515	0.467	0.653
A_3	0.597	0.511	0.524	0.588
A_4	0.575	0.539	0.449	0.679

TABLE XII
THE SCORE VALUES OF ALTERNATIVES FOR α_j AND β_j

Alternatives	α_j	β_j
A_1	0.697	0.553
A_2	0.544	0.407
A_3	0.543	0.468
A_4	0.518	0.385

$$X_{1b} = \frac{0.697}{0.518} + \frac{0.553}{0.385} = 2.783,$$

and

$$X_{1c} = \frac{0.5 \cdot 0.697 + (1-0.5)0.553}{0.5 \cdot 0.697 + (1-0.5)0.593} = 1.0.$$

Step 11: The assessment value X_j is found by (29) using the X_{ja}, X_{jb} and X_{jc} values in Table XIII and is presented in Table XIII. For example, the assessment value of A_1 can be calculated as follows:

$$X_1 = \sqrt[3]{0.304 \cdot 2.783 \cdot 1} + \frac{0.304 + 2.783 + 1}{3} = 2.308.$$

Step 12: The alternatives according to the decreasing value of X_j $(j = 1, 2, 3, 4)$ are ranked. A_1 is the best among the four OWF alternative sites, while A_4 is the worst.

A. Comparative Analysis

In order to test the rationality and effectiveness of the

TABLE XIII
THE RELATIVE SIGNIFICANCE AND THE FINAL RANKING OF THE OWF SITES

Alternatives	X_{ja}	X_{jb}	X_{jc}	X_j	Rank
A_1: Utsira Nord	0.304	2.783	1.000	2.308	1
A_2: Stadthavet	0.231	2.107	0.761	1.751	3
A_3: Frøyabanken	0.246	2.264	0.808	1.872	2
A_4: Træna Vest	0.219	2.000	0.722	1.662	4

TABLE XIV
COMPARATIVE ANALYSIS WITH OTHER Q-ROFSS BASED MCDM APPROACH

Techniques	A_1	A_2	A_3	A_4	Final Ranking
q-ROFSs based CoCoSo	2.308	1.751	1.872	1.662	$A_1 > A_3 > A_2 > A_4$
q-ROFSs based TOPSIS [77]	0.902	0.295	0.474	0.365	$A_1 > A_2 > A_3 > A_4$

proposed hybrid model, the ranking results are compared with Alkan and Kahraman's [77] q-ROFSs based TOPSIS approach. The ranking results are given in Table XIV. As can be seen, A_1 is the best alternative, while A_4 is the worst alternative. Considering the results obtained, it can be concluded that there are changes in A_2 and A_3 rankings as a result of different distance approaches in the application of the q-ROFSs-based TOPSIS approach and the process of the weighted decision matrix before normalization processs. The ranking results and reliability of the proposed hybrid model are also verified by the experts.

B. Checking the Stability of the Results

In most decision-making models, subjective parameters are defined based on the perception of the problem by the decision-maker and the risk that exists in the environment. Therefore, the values of these parameters are not unique, but their change depending on the conditions in which the decision-making system is modelled. Therefore, when making the final decision, it is necessary to answer the question: "Do subjectively defined parameters in the mathematical model have a decisive influence on the final results?"

In the FUCOM-CoCoSo q-ROF based model, three parameters (q, γ, and λ) have been identified, which are defined based on the subjective preferences of the decision-maker. In the next section, through three experiments, the dependence of the initial solution on the change of the parameters q, γ, and λ is presented. In the first two experiments, the influence of the parameters q and γ on the change in the values of the weighted q-ROF Hamacher function and the weighted strategy of the q-ROF CoCoSo model was analysed. In the third experiment, the influence of the parameter λ on the definition of compromise strategies of alternatives was analysed. In the following section, the described analysis is presented through the variation of the stated parameters.

1) Experiment 1 – Influence of parameter q on ranking results

When defining the initial solution, the experts adopted the value of the parameters $q = 1$. In the following section, the change of the parameter q in the interval $1 \leq q \leq 100$ is simulated. Fig. 11 shows the dependence of the integrated values of the q-ROF Hamacher function on the parameter q.

It can be seen from Fig. 11 that an increase in the parameter q in the interval $1 \leq q \leq 100$ affects the decrease in the integrated score function of alternative A_1. Furthermore, the remaining alternatives (A_2, A_3, and A_4) generally increase the value of integrated score functions. Since alternative A_1 is initially ranked first, such changes can lead to a change in

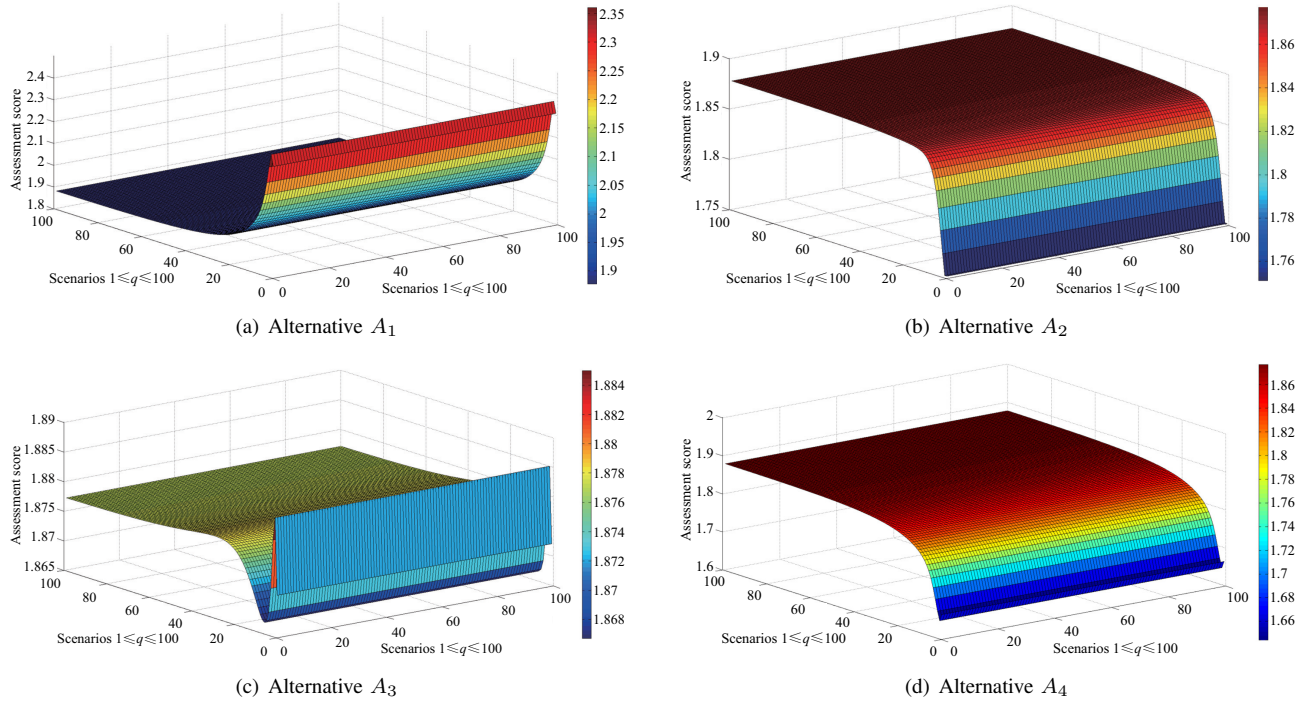

(a) Alternative A_1

(b) Alternative A_2

(c) Alternative A_3

(d) Alternative A_4

Fig. 11. Influence of parameter change $1 \leq q \leq 100$ on change of q-ROF Hamacher function.

initial rank, which is analysed in the following section. To see the influence of the parameter q on the difference in the rankings of alternatives, Fig. 12 shows a relative change in the integrated score functions of all alternatives.

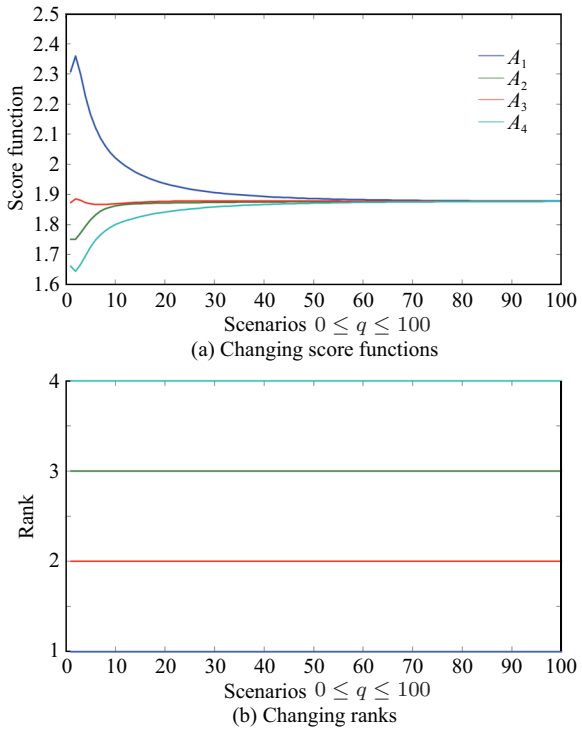

(a) Changing score functions

(b) Changing ranks

Fig. 12. Dependence of integrated score function alternatives on coefficient change $1 \leq q \leq 100$.

Changes in the parameter q through the considered 100 scenarios (Fig. 12(a)) influenced the change in the values of the integrated score functions as follows: $1.8777 \leq X_1 \leq 2.3077$, $1.7512 \leq X_2 \leq 1.8770$, $1.8719 \leq X_3 \leq 1.8770$, and $1.6624 \leq X_4 \leq 1.8766$. The results show that the increase in the parameter q affects the approximation of the criterion functions of the alternatives. Higher values of the parameter q lead to equalisation of alternatives, making it difficult to arrive at a final decision, while values of $1 \leq q \leq 15$ allow a clear definition of the advantages between alternatives. Therefore, it is recommended that when defining the initial solution, the parameter q be in the interval $1 \leq q \leq 15$. From the presented analysis, we can conclude that the initial rank $A_1 > A_3 > A_2 > A_4$ is confirmed (Fig. 12(b)), i.e., alternative A_1 is the dominant solution from the set.

2) Experiment 2 – Influence of parameters γ on ranking results

Changes in the value of γ affect the mathematical formulation of q-ROF Hamacher functions and change the integrated score strategies of alternatives (X_i). For the calculation of the initial solution, the value $\gamma = 1$ was arbitrarily adopted. Since this is a subjectively defined parameter, the following part analyses the impact of changing the parameter γ by 100 scenarios ($1 \leq \gamma \leq 100$). Fig. 13 shows the dependence of the q-ROF Hamacher function on the change of the parameter γ.

The parameter γ represents the stabilisation parameter of the q-ROF Hamacher function and significantly impacts the final

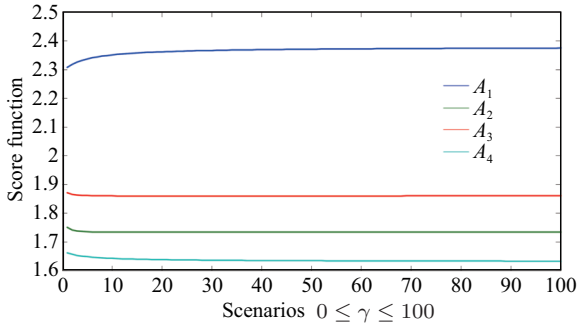

Fig. 13. Influence of parameter change $1 \leq \gamma \leq 100$ on change of q-ROF Hamacher function.

values of the integrated score strategies of the alternatives. Fig. 13 indicates that an increase in parameter $1 \leq \gamma \leq 100$ affects the increase in the integrated score function of alternative $A_1(2.3077 \leq X_1 \leq 2.3750)$. Furthermore, in all other alternatives, there is a decrease in the integrated score function. Since alternative A_1 is the first ranked, these results indicate that an increase in the value of the parameter γ leads to an increase in the advantage of alternative A_1 over the remaining alternatives in the set. With the remaining alternatives, there are no extreme changes in the values of the integrated score functions, which is confirmed by the following values $1.7351 \leq X_2 \leq 1.7512$, $1.8607 \leq X_3 \leq 1.8720$ and $1.6337 \leq X_4 \leq 1.6624$. Based on the presented values, we can conclude that the initial rank $A_1 > A_3 > A_2 > A_4$ is confirmed and the alternative A_1 represents the dominant solution from the considered set.

3) Experiment 3 – Influence of λ parameters on ranking results

The calculation of the integrated score functions in the q-ROF Hamacher CoCoSo model requires the definition of the value of the parameter λ. Based on the recommendations of Yazdani *et al*. [74] for calculating the initial solution, the value $\lambda = 0.5$ was adopted. This enabled weighted Hamacher functions to have an equal impact on defining the trade-offs of alternatives [74]. In the next part, 50 scenarios were formed through which the change of the parameter $0 \leq \lambda \leq 1$ was simulated. In the first scenario, the value $\lambda = 0$ was adopted, while in each subsequent scenario, the parameter value was increased by 0.02. The influence of the change of the parameter λ on the change of the integrated functions is shown in Fig. 14.

The results in Fig. 14 show that changing the parameter $0 \leq \lambda \leq 1$ does not lead to changes in the initial ranking of alternatives and that the initial ranking $A_1 > A_3 > A_2 > A_4$ is credible.

C. Offshore Energy-specific Results and Discussion

Companies planning such large-scale energy investments spend several months even years to make the most effective decisions for their investments. The decision-making process relies on various, mostly complex, investigations and analyses of various technical, economic, financial, environmental and political issues. Hence the demonstrated approach aims to simplify the decision-making process of the OWF investors.

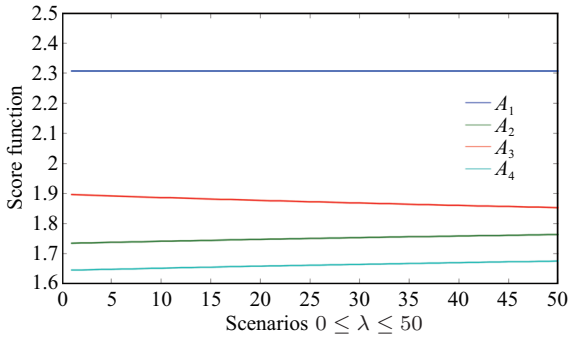

Fig. 14. The analysis of the influence of the parameter λ.

The easiest accessible information regarding any potential wind energy project and its location would be the wind speed values. If the investors proceed with a swift estimate and ranking using wind speed information, the order of the selected OWF locations would be as follows: $A_2 > A_1 > A_3 > A_4$. Net capacity factor is one of the most critical decision-making metrics used in the wind industry, among other similar metrics. All investigated OWFs have very high offshore wind potential with net capacity factors over 40%. If the decision was made according to only the capacity factor results, as indicated in Table II, the ranking would be as follows: $A_2 > A_1 > A_3 > A_4$. The net capacity factor depends on various factors, as mentioned in the previous sections. In this case, the ranking based on wind speed and net capacity factor yields the same results. Since the annual energy yield is also a derivative metric of the net capacity factor, the order based on these metrics would not change the results. The ultimate project investment decision relies on more sophisticated analyses and investigations that consider all the techno-economic and other criteria such as distance to the nearest grid connection point, water depth, ecological and environmental constraints which shall be considered integrally to give the best available decision in terms of the best OWF location and project. According to the results of the proposed approach, A_1 (Utsira Nord) ranked as the best and A_4 (Træna Vest) as the worst OWF among four alternatives. Again, according to Table XIII, A_3 (Frøyabanken) ranked second and A_2 (Træna) ranked third. Indeed, this ranking shall be understood as an example only and not as a conclusive ranking of the sites. It serves to illustrate the novel methodology described in this paper.

VI. Conclusion and Policy Implications

This study proposes an efficient q-rung orthopair fuzzy sets based on FUCOM and CoCoSo method for solving the floating OWF site selection problem in Norway. The proposed q-ROFSs based MCDM model is comprised of two main stages. In the first stage, the q-ROF FUCOM is used to calculate the weight coefficients of the criteria. In the second stage, q-ROF CoCoSo is applied to rank the OWF alternative sites in Norway.

Taking multiple technical, economic, environmental, and social criteria into account, the proposed decision-making approach was demonstrated to evaluate four potential Norwegian OWF sites where floating offshore wind turbines are eligible. If the proposed decision-making algorithm was executed, the ranking of the investigated OWF location alternatives would be $A_1 > A_3 > A_2 > A_4$.

Since the project investment volumes of offshore wind energy projects and the associated consequences of any failure or wrong estimations in decision-making are critical, it is vital to perform a detailed site selection methodology to make feasible investment decisions. The demonstrated methodology is proposed to serve as an advanced and practical decision-support tool when making project-related verdicts and choices. Depending on the use case, policy-makers may prefer to utilise such decision-support tools to investigate the feasibility of potential locations for commercial use.

Even though this study proposes new methods implemented in the Norwegian OWF context, it contains some limitations that offer further development opportunities in future research. Firstly, the decision-making model was applied to a single sector (i.e. energy) within a case study. Another limitation is the potential dependency and interaction between criteria not considered in the proposed model. A third limitation is the number of experts who are members of the decision-making committee. It is also possible to consider additional criteria such as detailed techno-economic metrics, for example the levelised cost of electricity (LCoE), or additional constraints like military zones and shipping routes. In future, the proposed MCDM model with q-rung orthopair fuzzy Einstein average (q-ROFEA) and q-rung orthopair fuzzy Einstein average (Wq-ROFEA) operators can be extended.

In Norway, at the moment, Utsira Nord is opened for the development of offshore wind farms. Several companies are interested in developing a floating wind farm at the site, and these will compete for the license issued by the Norwegian government. A possible alternative application of the methodology described is to modify it for the ranking of competitive bids.

Q-Rung orthopair fuzzy sets were used in this study to represent vagueness and uncertainty in expert estimates. In the q-ROFS approach, uncertainties in information are represented through the degree of membership and the degree of non-membership. For a more objective presentation of expert assessments in future research, linguistic estimates can be presented using three segments: the degree of membership, the degree of abstinence, and non-membership. Applying the T-spherical fuzzy approach, i.e., adding the degree of abstinence for presenting expert preferences, would objectify the multi-criteria framework and enable experts to more rationally express their judgements. Additionally, the decision-making problem may be expanded with Pythagorean fuzzy sets in the future.

The main limitation of methodology is the complex mathematical algorithm for the calculation of Hamacher functions. Changes in the values of the parameters q and Υ further complicate the application of this algorithm. This limitation can be eliminated by creating a user-friendly software solution that will allow a more comprehensive implementation of the presented algorithm to solve real-world problems. The authors developed a software solution using MATLAB and Microsoft

Excel software while working on this study. This solution was then used to validate the results shown in Section V-B.

REFERENCES

[1] IEA, "Offshore wind outlook 2019. World energy outlook special report," 2019.

[2] IRENA, "Future of wind: Deployment, investment, technology, grid integration and socio-economic aspects," 2019.

[3] Wind Europe, "Our Energy, Our Future. How offshore wind will help Europe go carbon-neutral," 2019.

[4] L. Ramirez, D. Fraile, and G. Brindley, "Offshore wind in Europe: Key trends and statistics 2019," 2020.

[5] Q. Liu, Y. Sun, and M. C. Wu, "Decision-making methodologies in offshore wind power investments: A review," *Journal of Cleaner Production*, vol. 295, pp. 126459, May 2021.

[6] Y. P. Wu, "Inflation with teleparallelism: Can torsion generate primordial fluctuations without local Lorentz symmetry?," *Physics Letters B*, vol. 762, pp. 157–161, Nov. 2016.

[7] B. Wu, T. L. Yip, L. Xie, and Y. Wang, "A fuzzy-MADM based approach for site selection of offshore wind farm in busy waterways in China," *Ocean Engineering*, vol. 168, pp. 121–132, Nov. 2018.

[8] M. Abdel-Basset, A. Gamal, R. K. Chakrabortty, and M. Ryan, "A new hybrid multi-criteria decision-making approach for location selection of sustainable offshore wind energy stations: A case study," *Journal of Cleaner Production*, vol. 280, pp. 124462, Jan. 2021.

[9] A. Gimpel, V. Stelzenmüller, B. Grote, B. H. Buck, J. Floeter, I. Núñez-Riboni, B. Pogoda, and A. Temming, "A GIS modelling framework to evaluate marine spatial planning scenarios: Co-location of offshore wind farms and aquaculture in the German EEZ," *Marine Policy*, vol. 55, pp. 102–115, May 2015.

[10] M. Vasileiou, E. Loukogeorgaki, and D. G. Vagiona, "GIS-based multi-criteria decision analysis for site selection of hybrid offshore wind and wave energy systems in Greece," *Renewable and Sustainable Energy Reviews*, vol. 73, pp. 745–757, Jun. 2017.

[11] D. Vagiona and N. Karanikolas, "A multicriteria approach to evaluate offshore wind farms siting in Greece," *Global NEST Journal*, vol. 14, no. 2, pp. 235–243, Mar. 2012.

[12] A. Fetanat and E. Khorasaninejad, "A novel hybrid MCDM approach for offshore wind farm site selection: A case study of Iran," *Ocean & Coastal Management*, vol. 109, pp. 17–28, Jun. 2015.

[13] M. Deveci, U. Cali, S. Kucuksari, and N. Erdogan, "Interval type-2 fuzzy sets based multi-criteria decision-making model for offshore wind farm development in Ireland," *Energy*, vol. 198, pp. 117317, May 2020.

[14] P. Ziemba, "Multi-criteria fuzzy evaluation of the planned offshore wind farm investments in Poland," *Energies*, vol. 14, no. 4, pp. 978, Feb. 2021.

[15] J. Y. Kim, K. Y. Oh, K. S. Kang, and J. S. Lee, "Site selection of offshore wind farms around the Korean peninsula through economic evaluation," *Renewable Energy*, vol. 54, pp. 189–195, Jun. 2013.

[16] T. Kim, J. I. Park, and J. Maeng, "Offshore wind farm site selection study around Jeju Island, South Korea," *Renewable Energy*, vol. 94, pp. 619–628, Aug. 2016.

[17] C. D. Yue and M. H. Yang, "Exploring the potential of wind energy for a coastal state," *Energy Policy*, vol. 37, no. 10, pp. 3925–3940, Oct. 2009.

[18] U. Cali, N. Erdogan, S. Kucuksari, and M. Argin, "Techno-economic analysis of high potential offshore wind farm locations in Turkey," *Energy Strategy Reviews*, vol. 22, pp. 325–336, Nov. 2018.

[19] M. Argin, V. Yerci, N. Erdogan, S. Kucuksari, and U. Cali, "Exploring the offshore wind energy potential of Turkey based on multi-criteria site selection," *Energy Strategy Reviews*, vol. 23, pp. 33–46, Jan. 2019.

[20] M. Deveci, E. Özcan, R. John, D. Pamucar, and H. Karaman, "Offshore wind farm site selection using interval rough numbers based Best-Worst Method and MARCOS," *Applied Soft Computing*, vol. 109, pp. 107532, Sep. 2021.

[21] A. D. Mekonnen and P. V. Gorsevski, "A web-based participatory GIS (PGIS) for offshore wind farm suitability within Lake Erie, Ohio," *Renewable and Sustainable Energy Reviews*, vol. 41, pp. 162–177, Jan. 2015.

[22] M. Deveci, N. Erdogan, U. Cali, J. Stekli, and S. Y. Zhong, "Type-2 neutrosophic number based multi-attributive border approximation area comparison (MABAC) approach for offshore wind farm site selection in USA," *Engineering Applications of Artificial Intelligence*, vol. 103, pp. 104311, Aug. 2021.

[23] A. Chaouachi, C. F. Covrig, and M. Ardelean, "Multi-criteria selection of offshore wind farms: Case study for the Baltic States," *Energy Policy*, vol. 103, pp. 179–192, Apr. 2017.

[24] C. Schillings, T. Wanderer, L. Cameron, J. T. van der Wal, J. Jacquemin, and K. Veum, "A decision support system for assessing offshore wind energy potential in the North Sea," *Energy Policy*, vol. 49, pp. 541–551, Oct. 2012.

[25] L. Cradden, C. Kalogeri, I. M. Barrios, G. Galanis, D. Ingram, and G. Kallos, "Multi-criteria site selection for offshore renewable energy platforms," *Renewable Energy*, vol. 87, pp. 791–806, Mar. 2016.

[26] M. Deveci, E. Özcan, R. John, C. F. Covrig, and D. Pamucar, "A study on offshore wind farm siting criteria using a novel interval-valued fuzzy-rough based Delphi method," *Journal of Environmental Management*, vol. 270, pp. 110916, Sep. 2020.

[27] L. A. Zadeh, "Fuzzy sets," *Information and Control*, vol. 8, no. 3, pp. 338–353, Jun. 1965.

[28] J. M. Mendel, "Type-2 fuzzy sets and systems: an overview," *IEEE Computational Intelligence Magazine*, vol. 2, no. 1, pp. 20–29, Feb. 2007.

[29] R. M. Rodriguez, L. Martinez, and F. Herrera, "Hesitant fuzzy linguistic term sets for decision making," *IEEE Transactions on Fuzzy Systems*, vol. 20, no. 1, pp. 109–119, Feb. 2012.

[30] Z. Pawlak, "Rough sets," *International Journal of Computer & Information Sciences*, vol. 11, no. 5, pp. 341–356, Oct. 1982.

[31] K. T. Atanassov, "Intuitionistic fuzzy sets," *Fuzzy Sets and Systems*, vol. 20, no. 1, pp. 87–96, Aug. 1986.

[32] L. A. Zadeh, "The concept of a linguistic variable and its application to approximate reasoning-III," *Information Sciences*, vol. 9, no. 1, pp. 43–80, 1975.

[33] J. M. Mendel, R. I. John, and F. L. Liu, "Interval type-2 fuzzy logic systems made simple," *IEEE Transactions on Fuzzy Systems*, vol. 14, no. 6, pp. 808–821, Dec. 2006.

[34] V. Torra, "Hesitant fuzzy sets," *International Journal of Intelligent Systems*, vol. 25, no. 6, pp. 529–539, Jun. 2010.

[35] R. R. Yager and A. M. Abbasov, "Pythagorean membership grades, complex numbers, and decision making," *International Journal of Intelligent Systems*, vol. 28, no. 5, pp. 436–452, May 2013.

[36] K. Ullah, "Picture fuzzy maclaurin symmetric mean operators and their applications in solving multiattribute decision-making problems," *Mathematical Problems in Engineering*, vol. 2021, pp. 1098631, Oct. 2021.

[37] T. Mahmood, K. Ullah, Q. Khan, and N. Jan, "An approach toward decision-making and medical diagnosis problems using the concept of spherical fuzzy sets," *Neural Computing and Applications*, vol. 31, no. 11, pp. 7041–7053, Nov. 2019.

[38] T. Mahmood, "A novel approach towards bipolar soft sets and their applications," *Journal of Mathematics*, vol. 2020, pp. 4690808, Oct. 2020.

[39] L. Wang and H. Garg, "Algorithm for multiple attribute decision-making with interactive Archimedean norm operations under Pythagorean fuzzy uncertainty," *International Journal of Computational Intelligence Systems*, vol. 14, no. 1, pp. 503–527, 2021.

[40] R. R. Yager, "Generalized orthopair fuzzy sets," *IEEE Transactions on Fuzzy Systems*, vol. 25, no. 5, pp. 1222–1230, Oct. 2017.

[41] R. R. Yager and N. Alajlan, "Approximate reasoning with generalized orthopair fuzzy sets," *Information Fusion*, vol. 38, pp. 65–73, Nov. 2017.

[42] A. Pinar and F. E. Boran, "A q-rung orthopair fuzzy multi-criteria group decision making method for supplier selection based on a novel distance measure," *International Journal of Machine Learning and Cybernetics*, vol. 11, no. 8, pp. 1749–1780, Aug. 2020.

[43] M. I. Ali, "Another view on q-rung orthopair fuzzy sets," *International Journal of Intelligent Systems*, vol. 33, no. 11, pp. 2139–2153, Nov. 2018.

[44] Y. Liu, G. Wei, S. Abdullah, J. Liu, L. Xu, and H. B. Liu, "Banzhaf-Choquet-copula-based aggregation operators for managing q-rung orthopair fuzzy information," *Soft Computing*, vol. 25, no. 10, pp. 6891–6914, May 2021.

[45] M. J. Khan, P. Kumam, and M. Shutaywi, "Knowledge measure for the q-rung orthopair fuzzy sets," *International Journal of Intelligent Systems*, vol. 36, no. 2, pp. 628–655, Feb. 2021.

[46] P. L. C. Van der Valk, "Coupled simulations of wind turbines and offshore support structures: Strategies based on the dynamic substructuring paradigm," Ph.D. dissertation, Technische Universiteit Delft, Delft, 2014.

[47] W. Beuckelaers, "Numerical modelling of laterally loaded piles for offshore wind turbines," PhD dissertation, University of Oxford, Oxford, 2017.

[48] E. Dupont, R. Koppelaar, and H. Jeanmart, "Global available wind energy with physical and energy return on investment constraints," *Applied Energy*, vol. 209, pp. 322–338, Jan. 2018.
[49] L. J. Vermeer, J. N. Sørensen, and A. Crespo, "Wind turbine wake aerodynamics," *Progress in Aerospace Sciences*, vol. 39, no. 6–7, pp. 467–510, Aug./Oct. 2003.
[50] A. C. Kheirabadi and R. Nagamune, "A quantitative review of wind farm control with the objective of wind farm power maximization," *Journal of Wind Engineering and Industrial Aerodynamics*, vol. 192, pp. 45–73, Sep. 2019.
[51] J. Meyers and C. Meneveau, "Optimal turbine spacing in fully developed wind farm boundary layers," *Wind Energy*, vol. 15, no. 2, pp. 305–317, 2012.
[52] M. Calaf, C. Meneveau, and J. Meyers, "Large eddy simulation study of fully developed wind-turbine array boundary layers," *Physics of Fluids*, vol. 22, no. 1, pp. 015110, 2010.
[53] M. R. Gustavson, "Limits to wind power utilization," *Science*, vol. 204, no. 4388, pp. 13–17, Apr. 1979.
[54] NVE, "Havvind. Forslag til utredningsomrader," 2010.
[55] NVE, "Havvind. Strategisk konsekvensutredning," 2012.
[56] NVE, "Svar pa oppdrag om apning av omrader for vindkraft til havs," 2017.
[57] "Havvind FRA Utsira og S0rlige NordsjII," In Norwegian. Accessed: 2021–09–07.
[58] Fiskeridirektoratet, "Fagrapport til strategisk konsekvensutredning av fornybar energiproduksjon til havs - Fiskeriinteresser," 2012.
[59] J. Smith, "Fagrapport til strategisk konsekvensutredning av fornybar energiproduksjon til havs - landskap, friluftsliv og reiseliv," 2012.
[60] A. Stormgeo, "Kraftproduksjon og vindforhold: Fagrapport til strategisk konsekvensutredning av fornybar energiproduksjon til havs," *Norwegian Water Resources and Energy Directorate*, 2012.
[61] S. P. Staffell and S. Pfenninger, "Renewables ninja," 2016.
[62] A. Martinez and G. Iglesias, "Multi-parameter analysis and mapping of the levelised cost of energy from floating offshore wind in the Mediterranean Sea," *Energy Conversion and Management*, vol. 243, pp. 114416, Sep. 2021.
[63] Floating Offshore Wind: Cost Reduction Pathways to Subsidy Free[Online]. [2021–10–05]. Available: https://ore.catapult.org.uk/wp-content/uploads/2021/01/FOW-Cost-Reduction-Pathways-to-Subsidy-Free-report-.pdf
[64] C. Maienza, A. M. Avossa, F. Ricciardelli, D. Coiro, G. Troise, and C. T. Georgakis, "A life cycle cost model for floating offshore wind farms," *Applied Energy*, vol. 266, pp. 114716, May 2020.
[65] M. Kausche, F. Adam, F. Dahlhaus, and J. Großmann, "Floating offshore wind - Economic and ecological challenges of a TLP solution," *Renewable Energy*, vol. 126, pp. 270–280, Oct. 2018.
[66] G. E. Jung, H. J. Sung, M. C. Dinh, M. Park, and H. Shin, "A comparative analysis of economics of PMSG and SCSG floating offshore wind farms," *Energies*, vol. 14, no. 5, pp. 1386, Mar. 2021.
[67] A. Ghigo, L. Cottura, R. Caradonna, G. Bracco, and G. Mattiazzo, "Platform optimization and cost analysis in a floating offshore wind farm," *Journal of Marine Science and Engineering*, vol. 8, no. 11, pp. 835, Oct. 2020.
[68] R. James and M. C. Ros, "Floating offshore wind: market and technology review," *The Carbon Trust*, vol. 439, 2015.
[69] Create a Box Plot[Online]. [2021-10-05]. Available: https://se.mathworks.com/help/stats/boxplot.html
[70] P. D. Liu and P. Wang, "Some q-rung orthopair fuzzy aggregation operators and their applications to multiple-attribute decision making," *International Journal of Intelligent Systems*, vol. 33, no. 2, pp. 259–280, Feb. 2018.
[71] G. W. Wei, H. Gao, and Y. Wei, "Some q-rung orthopair fuzzy Heronian mean operators in multiple attribute decision making," *International Journal of Intelligent Systems*, vol. 33, no. 7, pp. 1426–1458, Jul. 2018.
[72] X. D. Peng and J. G. Dai, "Research on the assessment of classroom teaching quality with q-rung orthopair fuzzy information based on multiparametric similarity measure and combinative distance-based assessment," *International Journal of Intelligent Systems*, vol. 34, no. 7, pp. 1588–1630, Jul. 2019.
[73] A. P. Darko and D. C. Liang, "Some q-rung orthopair fuzzy Hamacher aggregation operators and their application to multiple attribute group decision making with modified EDAS method," *Engineering Applications of Artificial Intelligence*, vol. 87, pp. 103259, Jan. 2020.
[74] M. Yazdani, P. Zarate, E. K. Zavadskas, and Z. Turskis, "A Combined Compromise Solution (CoCoSo) method for multi-criteria decision-making problems," *Management Decision*, vol. 57, no. 9, pp. 2501–2519, Oct. 2019.
[75] D. Pamučar, Ž. Stević, and S. Sremac, "A new model for determining weight coefficients of criteria in MCDM models: Full consistency method (FUCOM)," *Symmetry*, vol. 10, no. 9, pp. 393, Sep. 2018.
[76] H. Nguyen, "An application of intuitionistic fuzzy analytic hierarchy process in ship system risk estimation," *Journal of KONES*, vol. 23, no. 3, pp. 365–372, 2016.
[77] N. Alkan and C. Kahraman, "Evaluation of government strategies against COVID-19 pandemic using q-rung orthopair fuzzy TOPSIS method," *Applied Soft Computing*, vol. 110, pp. 107653, Oct. 2021.

Muhammet Deveci received the B.Sc. degree in Industrial Engineering from Cukurova University, Adana, Turkey, in 2010, the M.Sc. degree in Business Administration from the Gazi University, Ankara, Turkey, in 2012, and the Ph.D. degree in Industrial Engineering from Yildiz Technical University, Istanbul, Turkey, in 2017.

He is currently an Associate Professor with the Department of Industrial Engineering, Turkish Naval Academy, National Defence University, Istanbul, Turkey. He worked as a Visiting Researcher and Postdoctoral Researcher, in 2014–2015 and 2018–2019, respectively, with the School of Computer Science, University of Nottingham (UoN), Nottingham, U.K. He has authored/co-authored more than 50 international journal papers at reputable venues and about 30 conference papers. His research interests include computational intelligence, handling of uncertainty, multi-criteria decision-making, interval type-2 fuzzy sets, modelling and optimisation, and their hybrids, applied to complex real-world problems.

Dr. Deveci became the Guest Editors of many international journals such as the *IEEE Transactions on Fuzzy Systems*, the *International of Journal of Hydrogen Energy*, and the *Journal of Petroleum Science and Engineering*. He is the member of editorial boards of some international journals. He has served as a Reviewer for more than 60 journals.

Dragan Pamucar obtained his M.Sc. at the Faculty of Transport and Traffic Engineering in Belgrade in 2009, and his Ph.D. degree in Applied Mathematics with specialisation in Multi-Criteria Modelling and Soft Computing Techniques at University of Defence in Belgrade, Serbia in 2013.

Dr. Pamucar is an Associate Professor at the University of Belgrade, the Faculty of Organizational Sciences, Serbia. His research interest includes the fields of computational intelligence, multi-criteria decision-making problems, neuro-fuzzy systems, fuzzy, rough and intuitionistic fuzzy set theory, neutrosophic theory, with applications in a wide range of logistics problems. He has published 10 books and over 170 research papers in international scholarly academic journals.

Umit Cali (Member, IEEE) received the Ph.D. degree in Electrical Engineering and Computer Science from University of Kassel, Germany. He is currently an Associate Professor at the Department of Electric Power Engineering, Norwegian University of Science and Technology. His research interests include energy informatics, artificial intelligence, blockchain technology, renewable energy systems, and energy economics. He is the first author of Digitalization of Power Markets and Systems using Energy Informatics book. He is serving as the Chair of IEEE TEMS Special Interest Group on Energy DLT and the Vice Chair of IEEE Blockchain in Energy Standards WG (P2418.5).

Emre Kantar received the B.Sc. and M.Sc. degrees in Electrical and Electronics Engineering from the Middle East University (METU), Ankara, Turkey, in 2011 and 2014, respectively. From 2010 to 2014, he was working at Aselsan, Inc., Ankara, Turkey as an R&D engineer at the Department of Electronics Design. In 2019, he received the Ph.D. degree in Electric Power Engineering from Norwegian University of Science and Technology (NTNU), Trondheim, Norway. He is currently a research scientist at SINTEF Energy Research, Trondheim, Norway. His research interests include: condition-based & predictive maintenance methods for hydro-generator stator bars; electrical modelling and lifetime estimation of HV insulation materials and subsea connectors; battery management systems for EV and solar power applications; power electronics and renewable energy systems.

Konstanze Kölle received the B.Sc. degree in Mechanical Engineering and the M.Sc. degree in Chemical Engineering from RWTH Aachen University, Aachen, Germany, in 2012 and 2013, respectively. In 2018, she received the Ph.D. degree in Engineering Cybernetics from Norwegian University of Science and Technology (NTNU), Trondheim, Norway. She works currently as research scientist at SINTEF Energy Research in Trondheim, Norway. Her research interests include the design, operation and control of wind power plants, their integration into the power system and participation in electricity markets.

John O. Tande is Chief Scientist with SINTEF Energy Research. He is heading the sub-programme on offshore wind energy within the European Energy Research Alliance, and is member of the European Technology and Innovation Platform ETIP wind. In May 2019, at the ministerial meeting in Vancouver, he was awarded Mission Innovation Champion for his research achievements in offshore wind. Throughout his long and productive scientific career, he has made a significant contribution to the acceleration of the clean energy revolution in the field of offshore wind power, and floating wind farms in particular. Tande was the initiator and centre director for the research centre FME NOWITECH (2009-2017) that generated 40 innovations with a potential net present value of about 5,000 MEUR, and he is now centre director of the successor FME NorthWind (Norwegian Research Centre on Wind Energy, 2021-2029). He has published more than 100 articles (https://scholar.google.no/citations?hl=no&user=LKv1iPQAAAAJ). A key publication is the textbook “Offshore Wind Energy Technology” authored by Olimpo Anaya-Lara, John O. Tande, Kjetil Uhlen, Karl Merz and published by John Wiley & Sons Ltd, April 2018, 424 pp. It is based on research material developed in NOWITECH and comprises a comprehensive reference to the most recent advancements in offshore wind technology.